MINERALOGICAL MAGAZINE

VOLUME 54 NUMBER 374 MARCH 1990

S-type granite formation in the Dalradian rocks of Connemara, W. Ireland

Y. AHMED-SAID* AND B. E. LEAKE

Department of Geology and Applied Geology, University of Glasgow, Glasgow G12 8QQ, UK

Abstract

The vicinity of the 490 Ma Cashel gabbroic intrusion experienced pressures of about 4.05 ± 0.2 kbar and temperatures in excess of 850 °C. These conditions caused intense hornfelsing and partial melting of the surrounding Dalradian metasediments. From the study of the progressively changed composition of the aureole hornfelses it is deduced that elements were fractionated into the melts as follows: Si>K>Na>Ca>Mn>Al>Fe>Mg and Rb>Ba>Sr>Ga>Cr,Ni,Co. This order of fractionation, which is the opposite to that in magmatic crystallization, provides a detailed picture of the mode of interaction between a mantle derived basic magma and mid-crustal rocks, illustrating how one type of S-type granite can be produced. The rare earth elements (*REE*) were both removed and fractionated but Eu largely remained in the crystal fractions giving increasing positive Eu anomalies with rising partial melting and these trends can be explained by the extraction of a granitic melt from the hornfelses. Fission track mapping of U is used to study the behaviour of U within the aureole and the metamorphic recrystallization of detrital brown zircon to pink new zircon. The S-type Cashel microgranite sill is shown to have been derived by anatexis from the Dalradian rocks, to have preserved the Sr isotope ratios of the metasediments at 490 Ma, and not to be of the same composition as the leucosomes in the metasediments.

KEYWORDS: S-type granite, crustal melt, hornfelses, Dalradian, Ireland.

Introduction

THE Connemara metagabbroic-orthogneiss complex is the largest intrusion into the Dalradian rocks of Scotland or Ireland and extends for over 80 km in an E–W direction and over 25 km in a N–S direction (Leake, 1989). The Cashel part of the intrusion (Leake 1958*a*, 1970; see Fig. 1) displays the northern intrusive edge of the complex particularly well, with marked hornsfelsing and partial melting of the Dalradian metasediments (Leake and Skirrow, 1960; Evans, 1964; Ahmed-Said, 1988). The intrusion has been dated by zircon studies at 490 Ma (Jagger *et al.*, 1988) and provides an excellent example of the interaction of a mantle-derived magma with metasediments undergoing regional metamorphism and involving the production of a granitic magma by partial melting of metasediments. This magma is at least in part preserved in a microgranite sill segregated into a slip zone in the mobilized hornfelses.

Also in the same area in the Dalradian metasediments are leucosomes spatially associated with paleosomes which show no gradation into the microgranite and these have also been investigated. They are similar to those already studied by Barber (1985) and Barber and Yardley (1985) from east of the Cashel district and from which they deduced that leucosome melting and leucosome crystallization took place under different *P–T* conditions.

In view of recent experimental and theoretical modelling of the production of acid magma by melting adjacent to basaltic injections (Huppert and Sparks 1988), this area has been subjected to detailed study.

Mineralogical changes in the aureole

Pelites over 1.3 km from the intrusion typically contain 42% biotite, 26% plagioclase, 18% quartz, 4% fibrolite, 2% garnet, 0.38% opaque and very rare orthoclase, tourmaline and andalusite with common accessory apatite and zircon. Secondary sericite, chlorite and muscovite are ubiquitous. The modal mineralogy away from the intrusion (AA′ Figs 1 and 2) is compared with

* Now Department of Geology, Earth Sciences Institute, University of Annaba, Algeria

© *Copyright the Mineralogical Society*

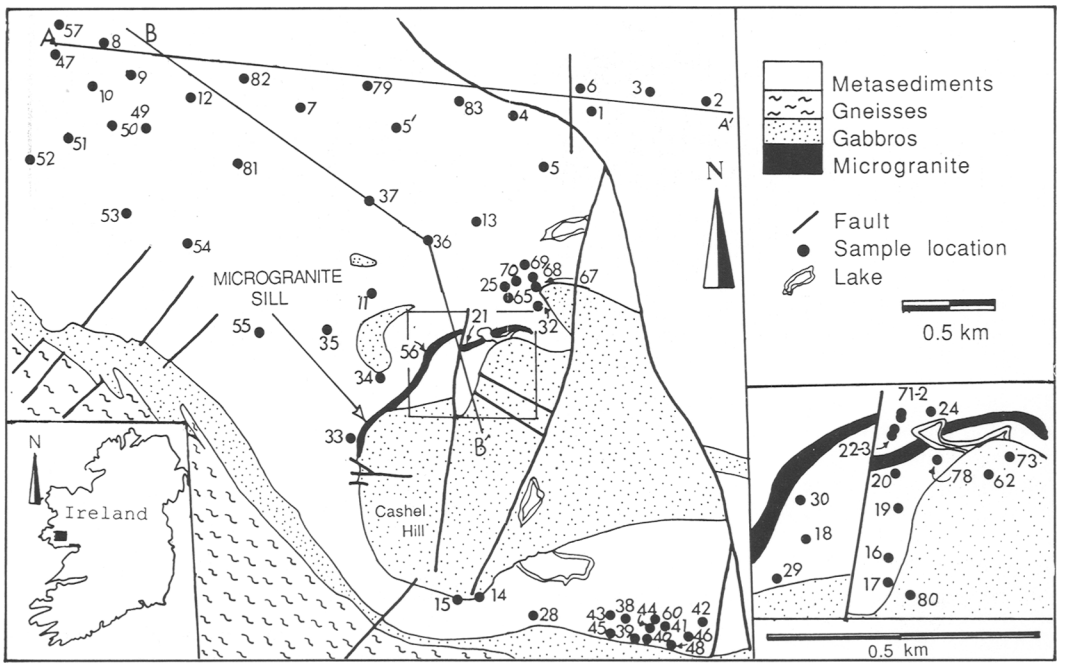

FIG. 1. Geological sketch map, after Leake (1970), showing sample locations and situation of the microgranite sill.

a N–S section (BB′, Figs 1 and 3) towards the intrusion. As Fig. 3 shows, the hornfels minerals cordierite, prismatic sillimanite, garnet, spinel, corundum and orthopyroxene are produced by reactions which involve quartz, biotite, fibrolite and plagioclase, the details of which can be found in Leake and Skirrow (1960). The most altered rocks are desilicated magnetite–spinel–corundum–orthopyroxene restite xenoliths.

Cordierite, which is recorded about 1.3 km from the contact and increases in size from 0.7 mm average diameter up to to 3 cm and in abundance up to 80%, largely grew at the expense of biotite but is usually strongly pinitized. Fresh relict cordierite has X_{Mg} [Mg/(Fe+Mg)] = 0.719, similar to analyses given by Evans and Leake (1970) and Treloar (1981). Prismatic sillimanite (1 mm average length), is recorded at 90–120 m from the contact and is always spatially associated with fibrolite, biotite, cordierite and garnet. Spinel, which appears as green droplets in garnet and cordierite, increases significantly both in size and abundance in the xenoliths and is usually magnetite coated. The spinel is pleonaste with Fe^{2+}/Mg ratios ranging from 1.05 to 0.74 indicating considerable substitution of Fe^{2+} for Mg. Corundum occurs as fresh, euhedral crystals and is found about a metre from the contact or in the xenoliths only. Orthopyroxene (0.18 mm average diameter) is restricted to the xenoliths. Magnetite increases markedly to values up to 38 times higher than in the unhornfelsed rocks. This increase of magnetite and that of spinel resulted in a "cellular" texture of magnetite and spinal.

Biotite is reduced drastically by replacement from 39% in the regional pelites to 14% or less in the pelitic xenoliths (Fig. 3). Recrystallized biotite forms large red poikiloblastic plates but the relicts are thin and mostly magnetite coated. There is a progressive colour change from red-brown in the country rocks to deep red, pale or black-oak brown in the innermost rocks or in the xenoliths. These changes in the colour of biotite are common in thermal aureoles and have long been attributed to an increase in Ti and Fe/Mg ratio (e.g. Tilley, 1924; Leake and Skirrow, 1960). However, microprobe analyses of biotites in 23 rocks ranging from unhornfelsed rocks through to xenoliths show that the Fe/Mg ratios decrease (Fig. 4A) with hornfelsing and as the biotite becomes redder. Ti has a wide range but redder biotites always yield higher Ti than the red brown ones within the same rock samples which indicates that Ti is the important element controlling the colour of these biotites.

Garnet is always almandine-rich and the four country rock garnets average Al_{75} Py_{13} Sp_9 Gr_3. These values are only slightly different from those

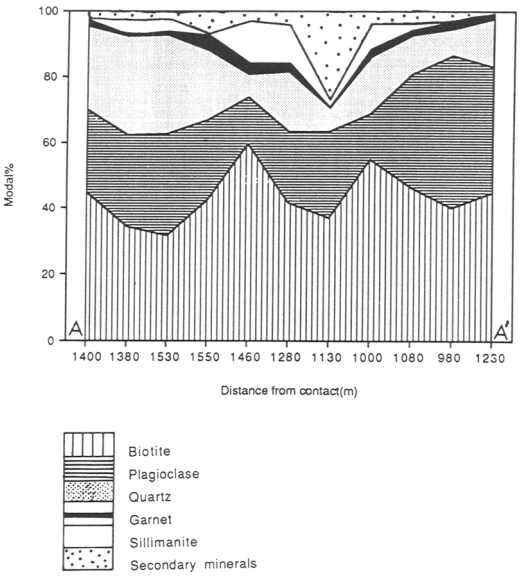

FIG. 2. Mineralogical cross section AA′ through the country rocks (see Fig. 1 for location).

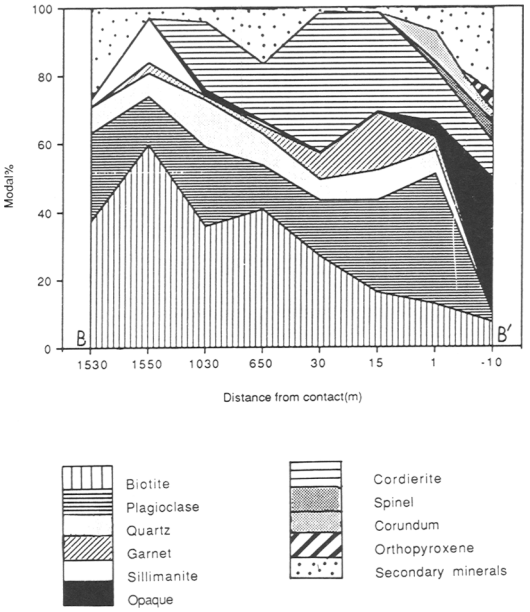

FIG. 3. Mineralogical cross section BB′ towards the intrusion (see Fig. 1 for location).

reported by Barber and Yardley (1985) of Al_{80} Py_{15} Sp_2 Gr_3. With hornfelsing, Mg increases, Mn decreases and Fe does not change until about a metre from the contact where it drops to its lowest values but Ca remains practically unchanged (Fig. 4B). Garnets are normally unzones but when zoning occurs it is limited to the outermost 0–200 μm rims (Fig. 5A). In the country rocks, zoning is characterized by lower Mg and higher Mn in the rims but Fe and Ca remain unchanged, a common pattern in high-grade metamorphic rocks (e.g. Grant and Weiblen, 1971). In the hornfelses, Fe enrichment at the rims is matched by a decrease in the Mg content but Mn and Ca remain unchanged (Fig. 5B). This zoning is probably due to retrograde reactions, possibly with cordierite, the rims of which have higher X_{Mg} than the cores (Treloar, 1981).

The plagioclase composition trend (Fig. 4C) is an increase in anorthite content; although some of the plagioclase in the xenoliths may have derived from the basic magma.

Geothermometry and geobarometry

Treloar (1981, 1985), using garnet–biotite–cordierite compositions, calculated temperatures of over 700 °C 3 km north of the Cashel intrusion to over 800 °C within 100 m of the contact, all at pressures of 4.5 ± 1 kbar. These estimates were corroborated by Barber and Yardley's (1985) leucosome–paleosome studies and the same three minerals have been used in the present work together with calculations based on physical cooling theory.

Geothermometry. 19 garnet–biotite pairs and one garnet–cordierite pair have been analysed and, based on the partitioning of elements, indicate temperatures of between 643 and 1081 °C, depending on which calibration is used (Table 3). That of Ferry and Spear (1978) has been rejected as it consistently yields higher temperatures than both the empirical calibrations of Thompson (1976) and Holdaway and Lee (1977) which two yield consistent results between garnet–cordierite and garnet–biotite geothermometers.

The effects of octahedral substitution of Mn and Ca in garnet and Ti, Fe^{3+} and Al^{IV} in biotite on the K_D can be significant and have been theoretically studied by Dallmeyer (1974). These effects have been tested in the studied aureole because of the changes in the chemistry of the minerals concerned and it is found that only X_{Ti}^{bio} and X_{Mn}^{gt} have significant effects on the K_D (Fig. 6A and B); contrary to the suggestion of Yardley *et al.* (1980) that the effects of X_{Mn}^{gt} are only detectable in garnets which are unusually rich in spessartine.

More recently, Hodges and Spear (1982) and Indares and Martignole (1985) produced modified calibrations accounting for Ti and Al substitutions

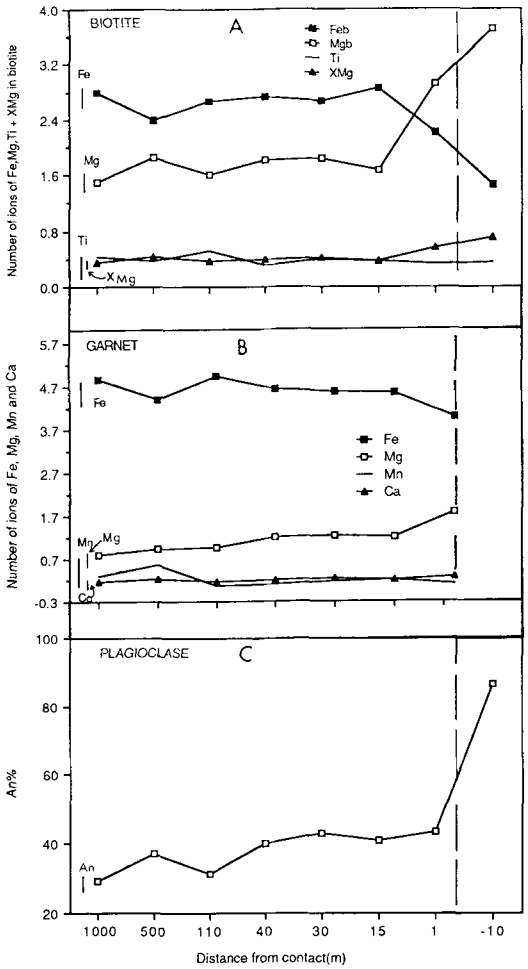

FIG. 4. Changes in the chemistry of biotite (A), garnet (B) and plagioclase (C) towards the intrusion (discontinuous line is the contact of the intrusion). Small bars on the left hand side represent the range of the elements concerned in the country pelites.

in biotite and/or Mn and Ca in garnet. Application of these two calibrations to the Cashel thermal aureole shows that the corrected calibration of Hodges and Spear gives only insignificant differences relative to the uncorrected forms of Thompson (1976) and Ferry and Spear (1978), whereas that of Indares and Martignole (1985) yields about 100 °C lower than the original temperatures derived using the original calibration of Ferry and Spear (1978). This trend is expected because $X_{(Ti+Al^{iv})}^{bio}$ is usually higher than 0.15, the upper limit that Ferry and Spear (1978) suggested for the use of their calibration without corrections. The widespread partial melting, however, suggests that many of the values of the Indares and Martignole (1985) calibration are too low, possibly because it was fitted to granulite facies rocks. It has therefore been rejected. The temperatures derived using the empirical calibration of Thompson (1976) are believed to be the best estimates of maximum temperatures and hence are shown in Fig. 7.

The cooling model of Carslaw and Jaeger (1947, 1959) and Jaeger (1958, 1959) has been used but its applicability was hindered by the substantial dehydration of the contact rocks, showing that heat was not transferred solely by conduction (Ahmed-Said, 1988). However, if the assumption that the heat effects of the volatile components and the latent heat of the solidifying magma equal those of the fluid derived from the melting metasediments, the temperatures derived show excellent agreement with those obtained from the uncorrected calibration of Thompson (1976) using garnet–biotite geothermometry. Taking the initial temperature (T_o) of the country rocks as 500 °C (Yardley *et al.*, 1987), Cashel pelites and semipelites as equivalent to 70% shale and 30% quartzite, the contact temperatures (T_c) are 880 and 766 °C for magma temperatures (T_m) of 1200 and 1000 °C respectively.

The method for calculating temperatures at different distances from the contact is given in Ahmed-Said (1988) and the thermal evolution of four points within the aureole for times from 0 to 20 000 years are shown in Fig. 8 for pure shales and taking $T_c = 930$ °C and $T_m = 1200$ °C. As is clear from this figure, at any distance $\leqslant 200$ m from the contact, the temperature should be $\geqslant 790$ °C which agrees well with the values shown in Fig. 7. The values of 670 and 695 °C obtained within this distance are low suggesting that some re-equilibration of minerals during cooling may have occurred, although due to contemporaneous and later tectonic events the present location of many samples relative to the contact may be different from the original one (Leake and Skirrow 1960).

Geobarometry. Garnet–aluminosilicate–quartz–plagioclase geobarometry was used as the main method to estimate the aureole pressures using the calibrations of Ghent (1976), Ghent *et al.* (1979) and Newton and Haselton (1981) including correction for the error in the last paper. Garnet–cordierite–sillimanite–quartz geobarometry as calibrated by Thompson (1976), Holdaway and Lee (1977) and Wells and Richardson (1980) has also been used. The Ghent (1976) calibration (Table 1) is rejected as it yields pressures about 1.2 kbar higher than that of Newton

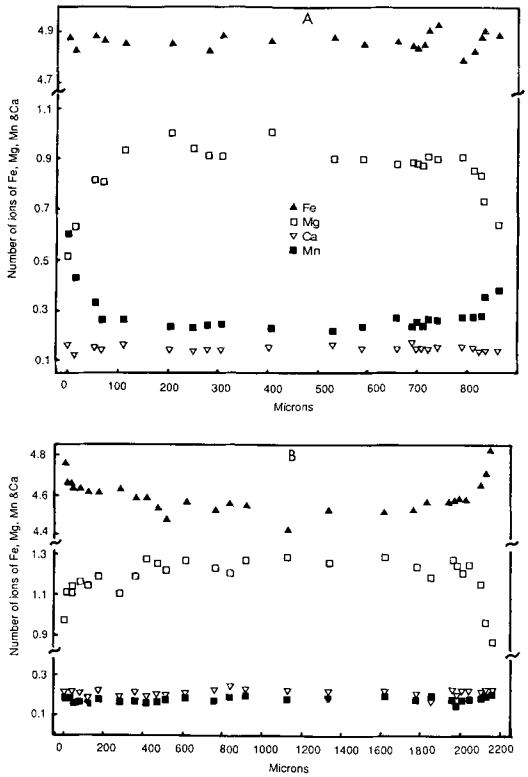

FIG. 5. Zoning patterns in garnet (A) from the country pelites and (B) hornfelsed rocks.

and Haselton (1981); this arises because only the latter accounts for the non-ideality of Ca in both garnet and plagioclase.

The estimates vary from 3.7 to 6.6 kbar with the highest pressures being recorded near the intrusion, but the most reliable value is that given by sample (Y55) because it yields the largest angle with the slope of the calibration (Fig. 9) suggesting a best estimate of 4.05 ± 0.2 kbar. This suggestion is supported by the similar pressures (4.5 ± 1 kbar) derived using garnet–cordierite–sillimanite–quartz barometry (Table 1; Treloar, 1985; Yardley, 1987).

Table 1: Temperatures and pressures derived using garnet-biotite geothermometry (in °C) and garnet-plagioclase geobarometry (in Kb)

Sample	Temperatures				Pressures	
number	K_D	H&L	F&S	T	G	N&H
Y4	3.284	724	811	766±16	5.5	4.25±0.27
Y5'	3.764	682	741	717 --	-	-
Y9	3.050	747	853	794±16	-	-
Y10	3.706	687	748	722±17	5.06	3.76±0.27
Y13	3.663	690	754	726±18	5.64	4.34±0.28
Y16	2.216	865	1081	940±35	7.61	6.69±0.49
Y17	2.987	757	865	803±18	6.86	6.24±0.26
Y19	2.540	811	973	873±80	6.91	5.98±0.11
Y20	2.582	805	962	866±26	6.59	5.61±0.37
Y23	3.341	643	676	670±7	-	-
Y42	3.942	669	719	701±42	-	-
Y49	3.123	740	839	785±45	6.16	4.97±0.70
Y50	3.018	751	859	799±25	-	-
Y53	3.715	686	747	721±19	5.17	3.89±0.28
Y55	2.932	760	877	810±16	5.11	4.05±0.22
Y65	4.011	664	711	695±16	-	-
Y70	3.570	698	767	735±30	-	-
Y72	3.050	747	853	794±35	5.35	4.22±0.51
Y79	3.03	749	857	797±49	6.44	5.59±0.79

Y17 (garnet-cordierite geothermometry); F&S = 746, T = 782

Y17 (garnet-cordierite barometry); H&L=4.63, T = 4.41, Wells and Richardson (1981) = 4.37

T = Thompson (1976); H&L = Holdaway and Lee (1977); F&S = Ferry and Spear (1978); G = Ghent (1976), N&H = Newton and Haselton (1981)

-- = not determined

Geochemistry

Major elements. The study of the fractionation of the major elements in the aureole is based on 13 country rock analyses in the present work and 34 southern Connemara pelites (27 from Senior and Leake, 1978; 7 from Leake, 1958*b*); 34 contact aureole samples by the present work plus 11 contact hornfelses (Leake and Skirrow, 1960) and nine pelitic xenoliths (6 from this work and 3 from Leake and Skirrow, 1960).

SiO_2 falls only slightly in the contact hornfelses but there is a marked fall in the xenoliths reaching an average of 19.95 ± 9.51 wt.% which should be compared to 54.9 ± 5.62 wt.% in the country rocks (Table 2). The extreme value is 9.54 wt.% SiO_2 for a sample reported by Leake and Skirrow (1960).

Na, K and P are clearly tending toward zero in some xenoliths, as biotite, feldspar and apatite were broken down and the released alkalis and P removed.

CaO decreases in the contact hornfelses before tending to rise to 2.84 ± 3.39 wt.% in the xenoliths. The good correlation of CaO with Na_2O (Fig. 10) indicates that Ca is being lost with Na in the melting of plagioclase, the melt being therefore higher in Na/Ca than the solid residue as is well established from the Ab–An liquid–solid equilibration diagram (Bowen, 1928). As a result, the An content of plagioclase increases from An_{28} in the country rocks to An_{74} in the xenoliths. Clearly some plagioclase entered the melts and the calculations performed below support this suggestion. The abnormally high wt.% CaO in some xenoliths [e.g. Y73 (8.72 wt.%), Y83 (8.18 wt.%)] is a marked reversal of the progressive loss of Na and Ca and is almost certainly

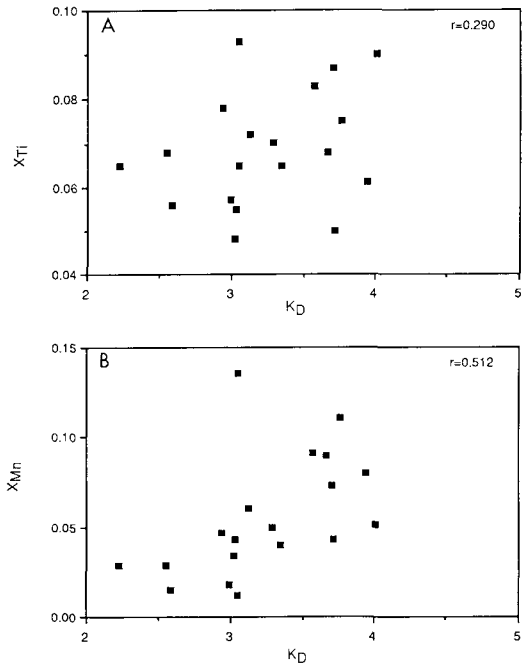

FIG. 6. Scatter diagrams of $X_{Ti^{bio}}$ (A) and $X_{Mn^{gt}}$ (B) *vs.* K_D.

due to the addition of plagioclase (bytownite)-forming material from the basic magma, a view confirmed by the similarity of plagioclase in these xenoliths to that in the basic rocks both as regards composition (An_{80-90}) and twinning (Carlsbad–albite twins).

Ti generally tends to rise and Zr falls in some xenoliths (Table 2, Fig. 11) which suggests that zircon was strongly melted out of the xenoliths but much of Ti was held in rutile, magnetite and spinel which must have had higher melting points than zircon.

Al, Mg and Fe_{tot} (as Fe_2O_3) increase progressively in the envelope hornfelses to concentrations in the xenoliths up to five times higher than in the country rocks for Fe_{tot} and twice for Mg and Al. This remarkable increase is caused by the melting out or breakdown and removal of quartz and feldspar and the breakdown of biotite and cordierite to magnetite, spinel and orthopyroxene in the xenoliths. This removes Si, Al, Na, K and Ca and leaves behind Fe, Mg and relatively increased Al. Fe^{3+} rises more rapidly than Fe^{2+} as the degree of hornfelsing rises, giving increasing oxidation ratio [mole Fe^{3+}/mole $(Fe^{3+} + Fe^{2+})$] towards the intrusion, which indicates that oxidizing conditions prevailed during the hornfelsing of the metasediments.

Trace elements. Rb, Ba and Zr change insignificantly in the envelope hornfelses then decline markedly in the xenoliths compared to the country rocks.

Sr decreases from 242 ± 64 ppm in the country rocks to 154 ± 90 ppm in the contact hornfelses before rising to 596 ± 386 ppm in the xenoliths. Sr isotope studies (Jagger, 1985) showed that there was some transfer of Sr from the basic magma into the metasediments and the rise in some xenoliths is probably due to this transfer, especially as some xenoliths do contain magmatic calcic plagioclase.

Ni, Co and Cr in the regional pelites rise strongly in the xenoliths, indicating that the femic elements are firmly held in high melting point minerals particularly orthopyroxene, magnetite, ilmenite and spinel.

Rare earth elements. *REE* analyses of four country-rock pelites, six pelitic hornfelses, two pelitic xenoliths, one xenolithic gabbro and one non-xenolithic gabbro are summarized in Table 3 and plotted in Fig. 12(A–C). There are three main features; variation in the total *REE* and in the $(La/Lu)_{CN}$ and Eu/Eu* ratios (Fig. 13).

The total *REE* decreases markedly from 315 ± 38 ppm in the regional pelites through 216 ± 27 ppm in the envelope hornfelses to 67.5 ± 9 ppm in the pelitic xenoliths. However the loss of the *HREE* is swifter and more pronounced than the *LREE* thus steepening the distribution patterns and there is an exceptionally high $(La/Lu)_{CN}$ ratio of 65.6 ± 17.22 in the xenoliths which should be compared to 11.24 ± 0.82 in the regional pelites. Previous work (e.g. McCarty and Kable, 1978; Henderson, 1984; Taylor and McLennan, 1985) showed that *HREE* are particularly enriched in zircon, apatite, garnet and orthopyroxene. In the Cashel metasediments zircon and apatite were probably the main control because of the good positive correlation of Lu with Zr and P (Fig. 14A and B) but rocks with similar proportions of garnet e.g. Y19 (7.46%) and Y69 (6.40%) yield considerably different patterns (Fig. 12B). The particularly high $(La/Lu)_{CN}$ ratio in the pelitic xenoliths is probably due to the melting of zircon and apatite with the released *HREE* not being appreciably accommodated in the orthopyroxene within the xenoliths. Sample Y69 has a remarkably high $(La/Lu)_{CN}$ ratio despite being rich in pink zircons, which suggests the metamorphic recrystallization of brown zircons not only released U to the melts (see below) but probably also *HREE*. This therefore indicates that the concave-shaped distribution patterns exhibited by some hornfelses in Fig. 12B reflect different proportions of pink and deep brown zircons.

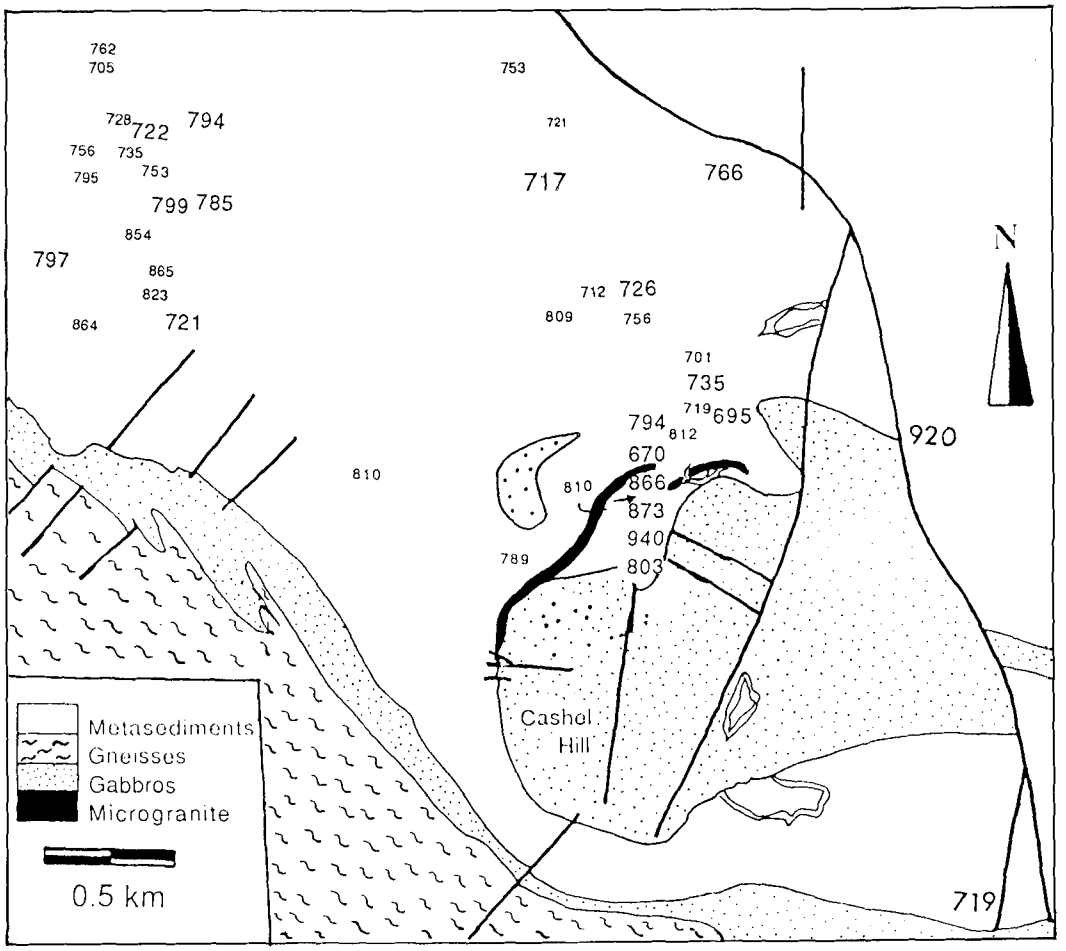

FIG. 7. Distribution of the temperatures derived using the calibration of Thompson (1976) of garnet–biotite thermometry. The small numbers are taken from Treloar (1985)

The Eu/Eu* ratio increases from consistently less than unity in the regional pelites through to consistently above unity in the pelitic xenoliths, indicating insignificant removal of Eu (Fig. 13). The positive Eu anomalies in the pelitic xenoliths cannot have originated from the basic magma for the following reasons: first, abnormally high Ca and eventually Sr are always accompanied by very low Eu contents (Fig. 14C and D); second, the pelitic restites Y68 and Y69 both have Eu/Eu*>1 but are far from the basic rocks (Fig. 1); and third, both xenolithic and non-xenolithic metagabbros exhibit practically the same *REE* distribution pattern (Fig. 12C). Probably a granitic melt has left the pelitic xenoliths and some of the strongly partially melted hornfelses, thereby becoming depleted in the other *REE* relative to Eu. The positive Eu anomaly may have partly resulted from the oxidation of Eu^{2+} into Eu^{3+}. Mass balance calculations showed that the material removed from the contact hornfelses and xenoliths always has a negative Eu anomaly which support this interpretation (Ahmed-Said, 1988). The microgranite sill (Fig. 12D) has a week negative Eu anomaly. The positive Eu anomalies in the lower continental crust (e.g. Rogers, 1977; Drury, 1978) have been interpreted by Taylor and McLennan (1985) as being residual in character, consistent with the above interpretation.

Spatial distribution of uranium. In the Cashel pelites U occurs in a variety of minerals including zircon, apatite, and biotite, and in grain boundaries, mineral fractures, alteration products, and along the schistosity planes. This indicates that garnet, quartz, feldspar, cordierite, orthopyroxene and magnetite are very low in U.

In the altered minerals and alteration products U is restricted to sericitized plagioclase, biotite

Table 2: Summary statistics of the major and trace elements of the pelites, and pelitic hornfelses.

	1		2		3		4	
Major elements	x	σ	x	σ	x	σ	x	σ
SiO_2	54.90	5.62	55.87	5.47	48.84	7.85	19.95	9.51
TiO_2	1.28	0.36	1.15	0.38	1.55	0.56	2.34	1.48
Al_2O_3	19.69	3.34	19.08	2.61	22.72	5.14	35.08	9.43
Fe_2O_3	2.19	1.3	1.58	0.44	2.49	1.61	12.1	5.25
FeO	6.92	2.67	7.06	1.45	9.03	2.65	13.6	4.16
MnO	0.22	0.16	0.16	0.07	0.17	0.07	0.17	0.06
MgO	3.31	1.03	3.29	0.61	4.19	1.39	7.14	2.07
CaO	1.93	1.07	1.51	0.52	1.34	1.33	2.84	3.39
Na_2O	2.24	0.92	2.5	1.00	1.33	0.72	1.06	1.00
K_2O	3.78	1.23	3.89	1.58	3.47	1.39	0.87	0.65
P_2O_5	0.2	0.19	0.13	0.10	0.10	0.07	0.04	0.02
Trace elements								
Rb	117	39	134	39	115	35	35	15
Ba	891	404	901	302	1057	375	680	20
Zr	272	46	236	69	259	85	120	43
Sr	242	64	203	64	154	89	596	386
Ga	27	5	27	4	33	8	74	20
Ni	48	11	57	13	72	22	173	59
Co	23	7	23	8	33	10	101	28
Cr	109	11	125	21	151	52	388	158
U	2.62	0.5	2.33	0.74	1.93	0.13	0.52	0.13
Th	10.8	2.4	13.48	2.5	13.9	5.2	2.3	0.8
Th/U	4.25	0.79	6.35	2.21	8.44	3.56	4.38	0.81
Th/K	3.73	1.6	3.9	1.78	3.96	2.04	2.38	1.62
U/K	0.87	0.39	0.72	0.5	0.59	0.34	0.50	0.26

1= average of country rocks (47 for major, 13 for trace elements, 11 for U and Th)

2= average of intermediate hornfelsed rocks (17 for both major and trace elements, 14 for U and Th)

3= average of contact hornfelsed rocks (45 for major, 34 for trace elements, 23 for U and Th)

4= average of xenoliths (9 for major , 6 trace elements, 5 for U and Th).

Table 3: Summary statistics of the REE of the regional pelites, hornfelses, gabbros and microgranite sill

	1		2		3		4	5	6
	x	σ	x	σ	x	σ			
La	66.53	15.0	49.07	17.3	18.78	4.9	26.11	32.16	45.61
Ce	130.9	30.1	91.86	25.6	29.59	8.4	61.23	73.65	99.05
Pr	16.12	4.1	10.92	3.8	3.02	0.8	7.79	9.17	10.8
Nd	61.51	12.8	40.9	17.0	11.74	3.4	35.36	41.93	45.04
Sm	10.38	2.3	6.21	2.9	1.44	0.4	6.26	7.77	7.08
Eu	2.11	0.2	1.52	0.5	0.77	0.1	1.21	1.91	1.52
Gd	8.77	2.0	5.04	2.4	1.04	0.3	5.07	6.39	5.22
Dy	7.54	1.7	4.03	2.1	0.49	0.1	3.51	4.63	2.86
Ho	1.73	0.4	0.91	0.5	0.09	0.02	0.74	1.04	0.58
Er	4.86	1.1	2.61	1.4	0.39	0	2.08	2.73	1.64
Yb	4.23	0.1	2.57	1.1	0.21	0.02	1.48	2.10	1.06
Lu	0.61	0.1	0.41	0.1	0.03	0	0.21	0.30	0.18
ΣREE	315.3	38.3	216.05	27.1	67.59	9.1	151.05	183.78	220.64
Eu/Eu*	0.71	0.17	1.13	0.73	2.02	0.30	0.65	0.82	0.76
(La/Lu)CN	11.24	0.82	12.64	1.62	65.59	17.22	12.91	11.13	26.33

1= average of 4 country rocks

2= average of 6 hornfelsed rocks

3= average of 2 pelitic xenoliths

4= 1 xenolithic metagabbro (J002 = Jagger 1985)

5= 1 non-xenolithic metagabbro (GJ009=Jenkin 1988)

6= microgranite sill

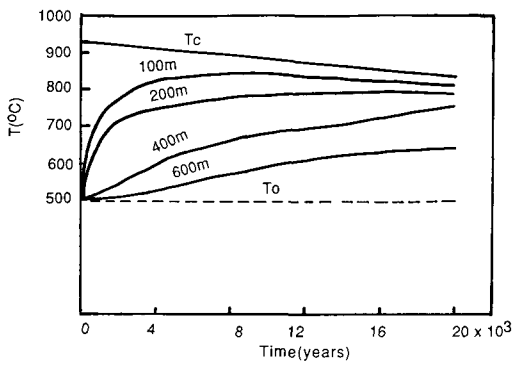

FIG. 8. Thermal evolution of four points within the aureole with time for pure shales and assuming the magma temperature (T_m) equals 1200°C. T_c = temperature at the contact and T_o = initial temperature of the country rocks at the time of the intrusion.

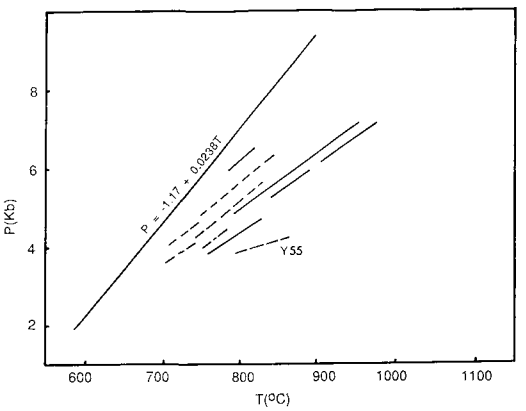

FIG. 9. P(kbar) *vs.* T(°C) to show the pressure dependence of the temperature. The slope of the Newton and Haselton calibration (1981) is labelled with the equation. Dashed line = country rocks; continuous line = hornfelsed rocks.

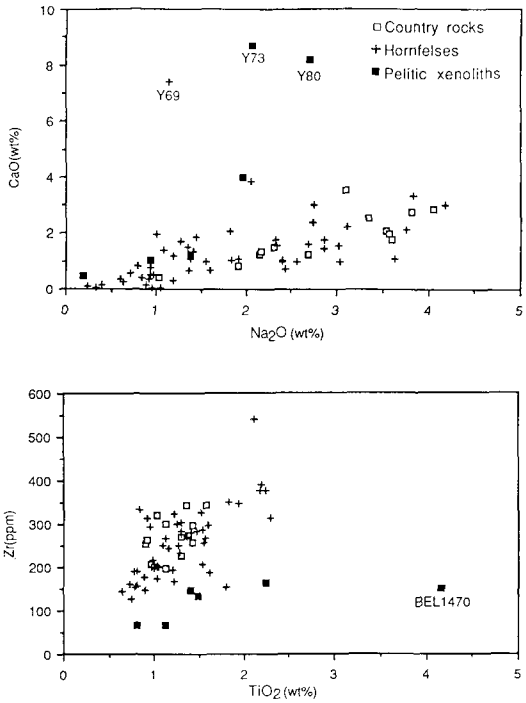

FIGS 10 and 11. FIG. 10 (top). Scatter diagram of CaO *vs.* Na_2O. Note the abnormally Ca-rich xenoliths (Y73 and Y80). Y69 is rich in Ca due to secondary prehnite rather than plagioclase. FIG. 11 (bottom). Scatter diagram of TiO_2 *vs.* Zr (note the Ti-rich but Zr-poor pelitic xenolith BEL1470). Symbols as in Fig. 10.

and garnet; the density of the fission tracks is directly proportional to the degree of alteration of the rocks, suggesting that this type of U is secondarily added and/or redistributed, the main source probably being alteration of biotite. In fractured minerals U is detected in garnets only. 200 analysed fresh unfractured and virtually inclusion-free garnet mounts were found to be U-free indicating that U along the fractures is related to sericite. It is also richest in the most micaceous pelites.

Zircon included in biotite, cordierite, garnet or plagioclase, has great inhomogeneities in both U contents and distribution patterns. More than 300 zircons were hand picked at random from samples occurring at different distances from the intrusion for shape, colour, surface abrasion, overgrowth and fission track (FT) studies.

Brown zircons ($\leq 90\,\mu m$), are frequently rounded to subrounded and always show typically pitted and abraded surfaces, even grains from rocks near the intrusion. These signs, which indicate mechanical abrasion during transport, can be regarded as good evidence that no later overgrowth or resorption took place and hence suggest a detrital origin for this group of zircons, a fact supported by the dominance of brown zircons in the country rock pelites and their extremely high U contents (see Fig. 15A). Pink zircons ($\geq 60\,\mu m$, Fig. 15C) are more euhedral, exhibit complex facetting with intact shining surfaces and have well preserved terminations on one end and sometimes on both ends. The remaining zircons examined are intermediate in colour, shape, and U contents between deep brown and pink zircons (Fig. 15B).

The grain size and number of euhedral zircons increase systematically towards the intrusion. The country rocks are dominated by brown zircon but nearer the intrusion euhedral pink zircons dominate (Fig. 16) and the more euhedral the crystal the greater the size. All this suggests that pink zircons are due to metamorphic recrystallization of brown ones.

The density of the fission tracks in the zircons depends on their colours, the deeper the colour the higher the density. Brown zircons have uniform FT distribution patterns and accommodate very large quantities of U which exhibits a star-like pattern (Fig. 15A). Pink zircons show great inhomogeneities in the distribution of U but in most cases the inhomogeneities show a regular pattern, being dense at the rims, two ends and along fractures, but scattered in the cores (Fig. 15C). The tendency of U to be more concentrated at the rims, which is regularly seen among the pink zircons, has probably resulted from the process of recrystallization, with U gain by equilibration with the environment. The mechanism(s) of uptake of U by zircons is difficult to define reliably but absorption through their external microfractures seems to be a typical property of the fractured surfaces of the grain which allow the penetration of U through thin cracks (Grauert *et al.*, 1974). Although no microcracks were seen and U is not obviously distributed along channels, an inward diffusion through the microcracks is regarded as most probable because unrecrystallized zircons from elsewhere also display this U distribution pattern (Ahmed-Said, 1988, p. 302).

In *biotite* U occupies three main sites; in zircon inclusions, absorbed onto the surfaces and in the lattices. In the crystal lattices, the presence of U is favoured by the large ionic radii positions available within biotite and is revealed by single, uniformly distributed FT which range in density from 0.76×10^4 to 3.25×10^5 t cm^{-2} giving U concentrations of between 0.09 and 3.25 ppm.

Apatites whatever their crystal shape, size and mounting positions always exhibit the same

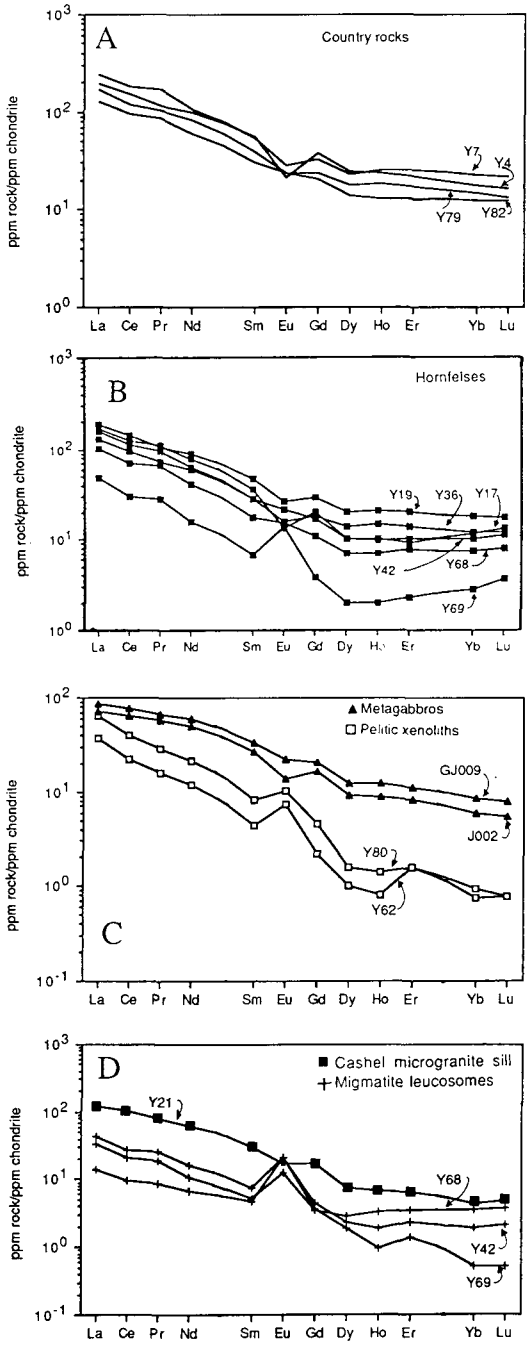

FIG. 12. *REE* distribution patterns in (A) the country rocks, (B) hornfelses (C) pelitic xenoliths and metagabbros (J002 = Jagger, 1985; xenolithic. GJ009 = Jenkin, 1988; non-xenolithic), (D) leucosomes and microgranite sill.

pattern of U distribution, being uniformly distributed throughout the whole crystals. The FT density varies from 0.75×10^6 to 5.59×10^6 t cm^{-2} giving U contents of between 7.64 and 57.90 ppm. This particularly wide range, coupled with the relatively large variations of U within the same samples, suggests that recrystallization of apatite is probable.

Quantitative estimation of U and Th. 53 samples have been analysed using instrumental neutron activation analysis (INAA) at the Scottish Universities Research and Reactor Centre (SURRC) (Table 2) with a precision less than 4% for both U and Th and an accuracy better than 1% for U and 4% for Th (Ahmed-Said, 1988).

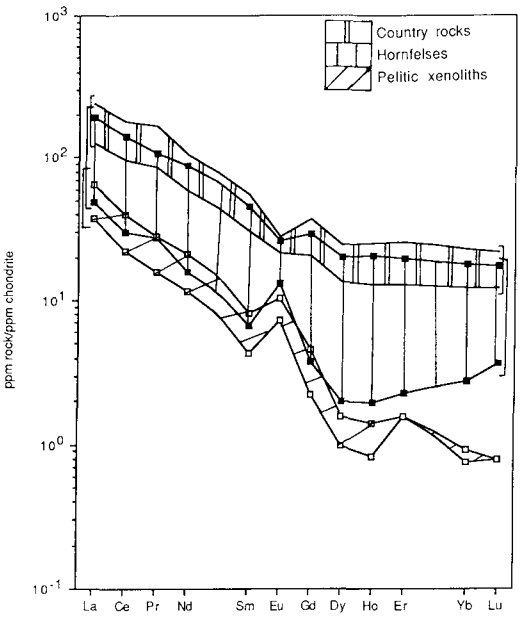

FIG. 13 Summary of the *REE* distribution patterns in the country and hornfelsed rocks and pelitic xenoliths. Note the systematic decrease in the ΣREE and increase in the Eu/Eu* and $(La/Lu)_{CN}$ ratios with rising hornfelsing.

The regional pelites average 2.62 ± 0.5 ppm U, 10.80 ± 2.39 ppm Th and 4.25 ± 0.79 Th/U ratios (Table 2, Fig. 17A). These values are similar to their equivalents in sedimentary shales (excluding black shales) of 3.7 ± 0.50 ppm U, 12.1 ± 1 ppm Th and 3.8 ± 1.1 Th/U ratio (Heier and Adams, 1965) indicating that the sedimentary signature was not significantly affected during regional metamorphism. However, unlike Th, U tends to be lower in the pelites than in common sedimentary shales consistent with the greater mobility

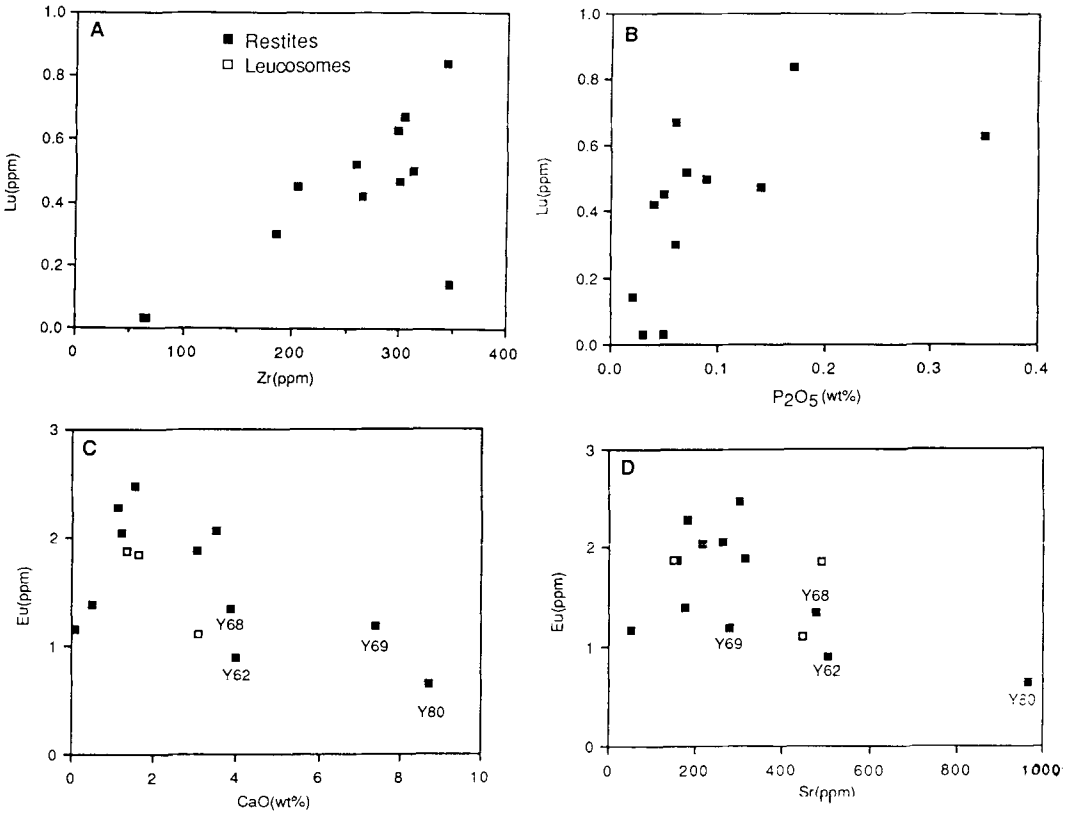

FIG. 14. Scatter diagrams of (A) Lu *vs.* Zr, (B) Lu *vs.* P_2O_5, (C) Eu *vs.* CaO, and (D) *vs* Sr for restites and leucosomes.

during surface chemical weathering and leaching of U rather than Th under supergene conditions.

U exhibits positive correlations with Zr and P (Fig. 17B and C) consistent with FT mapping of U where this is mostly held in zircon and apatite. In the pelitic xenoliths, only Zr shows a positive correlation with U and this is due to the substantial melting of apatite and the complete recrystallization of biotite releasing U to the outgoing melts. A contact hornfels (Y15) plots in the U-poor side of the diagram despite being rich in pink zircon and this is caused by the recrystallization of U-rich brown zircons into U-poor pink ones as discussed above.

Th correlates positively with K but not with Zr and P (Fig. 17D, E, F) indicating that Th is essentially held in biotite and possibly in pinitized cordierite and sericite but not in zircon and apatite, thus keeping similar Th values throughout the whole aureole.

U generally decreases as the intrusion is approached but Th remains unchanged until the xenolithic stage is reached where both elements decline to their lowest values of 0.52 ± 0.13 and 2.30 ± 0.83 ppm respectively (Table 2). As a result the Th/U ratios tend to rise from 4.25 ± 0.79 in the country pelites through 6.35 ± 2.21 in the intermediate hornfelses to 8.65 ± 3.25 in the contact areas before falling back to an average of 4.38 ± 0.87 in the pelitic xenoliths. Fig. 18 excludes the Th/U ratio being due to low-temperature mobilization and oxidation of U compared to Th, indicating that the increasing Th/U ratio towards the intrusion is due to primary fractionation between the two elements.

Cashel microgranite and the calculated compositions of melts removed from the hornfels

The Cashel microcline-rich microgranite sill, traceable along the northern edge of Cashel Hill (Fig. 1) was proposed by Leake (1970) to represent the segration of liquid derived from the partially melted metasediments along a curved

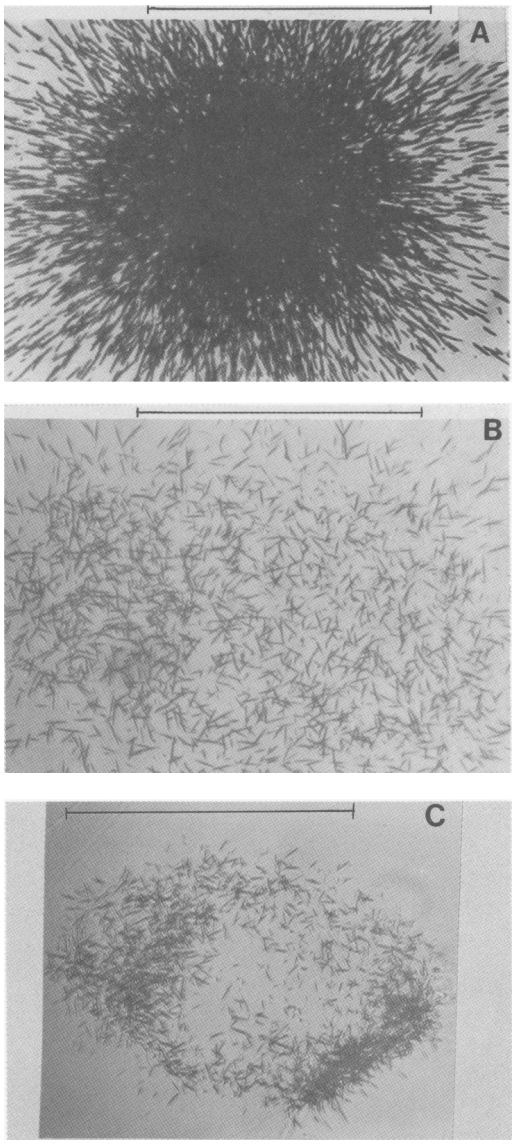

FIG. 15. Fission tracks in (A) brown zircon, (B) intermediate zircon and (C) pink zircon. Bar = 90μm.

surface of decollement during the southerly displacement of the Cashel body. The microgranite sill, which is composed of 33% microcline, 30% plagioclase, 26% quartz, 6% biotite and 4% secondary minerals, extends over one kilometer in a NE direction and varies in width from a few metres to over ten metres. Leake (1970) also favourably compared the major elements of the sill with the average composition of the melts derived from four pelitic xenoliths calculated by Leake and Skirrow (1960) and Evans (1964). However, these early calculations were strongly affected by the small sample size available to the authors and the absence of any isotopic results, and a more rigorous appraisal is now possible.

The femic elements such as Mg, Fe, Ti, Cr, Ni, Co and V enter the early-formed melts only slightly until very high temperatures are reached and hence can be used to ascertain the composition of melts derived from partially melted rocks assuming none of these elements enter the melts initially. Using the method described in Ahmed-Said (1988) Cr, Ni and Co (which are particularly refractory) have been used to estimate the compositions of the material melted out of the pelitic xenoliths and the order of fractionation of elements into the melts. The procedure first calculated an average country rock composition, a series of intermediate hornfels compositions based on comparable Cr, Ni or Co values and finally an average xenolith composition. By comparing the various intermediate hornfels and

Table 4: Calculated fractionation of the elements in the Cashel aureole (computed using Cr)

	1	2	P1	P2	P3	P4	P5	P6
SiO_2	56.70	20.63	91.38	87.99	84.06	76.87	73.67	70.77
TiO_2	1.33	2.42	0	0	0.45	0.68	0.82	0.90
Al_2O_3	20.33	36.28	0	0.72	4.22	10.81	12.83	14.12
Fe_{tot}	9.59	28.14	0	0	0	0	0.86	2.34
MnO	0.23	0.17	0.23	0.27	0.26	0.26	0.26	0.25
MgO	3.42	7.39	0	0	0.29	1.08	1.55	1.87
CaO	1.99	2.94	0	0.72	1.19	1.41	1.54	1.62
Na_2O	2.31	1.09	3.90	3.33	3.17	2.99	2.88	2.80
K_2O	3.90	0.90	7.12	6.62	6.05	5.60	5.32	5.07
P_2O_5	0.20	0.04	0.37	0.35	0.32	0.30	0.27	0.26
Total	100	100	100	100	100	100	100	100
Cr	109	388	0	0	0	0	0	0
Ni	48	173	0	0	0	0	0	0
Co	23	101	0	0	0	0	0	0
Ga	27	74	0	0	0	0.81	6	9
Sr	242	596	0	0	0	38	80	102
Zr	272	120	685	457	391	360	342	332
Ba	891	658	1525	1174	1073	1026	998	983
Rb	117	35	340	217	181	165	155	150

1 is the average of 47 country rocks (Table 2) recalculated to 100%.
2 is the average of 9 pelitic xenoliths (Table 2) recalculated to 100%.
P1 to P5 = are degrees of partial melting at 0.27, 0.45, 0.56, 0.63, 0.69 and 0.71 respectively. Note that the calculations are from P=0 to the degree of partial melting stated (i.e. P=0 to P=0.27, P=0 to 0.45 etc.)

xenolith averages with the country rock average, the composition of the removed material at various stages can be calculated and also the degree of partial melting assuming no Cr, Ni or Co enter the melts.

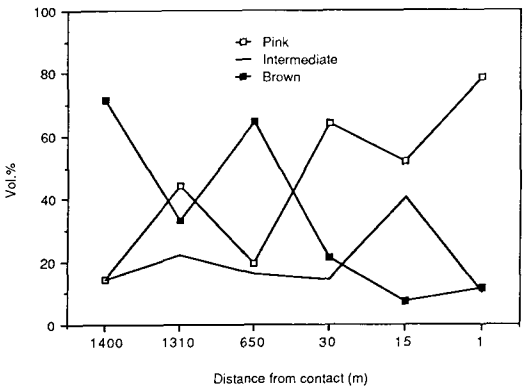

FIG. 16. Changes in the volume % of the different types of zircon towards the intrusion with pink varieties increasing and brown declining.

Table 4 shows that major and trace elements were fractionated into the melts as follows; Si>K>Na>Mn>Ca>Al>Mg>Fe and Rb>Zr>Ba>P>Ti>Sr>Ga>Cr,Ni,Co. If small amounts of Ca are subtracted from the average xenoliths to account for Ca coming mainly in magmatic calcic plagioclase, Ca would have entered the melts just after Na. Fe would have entered the melts before Mg because the high values in the xenoliths are due to Fe_2O_3 rather than FeO (Fe^{3+}/Fe^{2+} + 0.43 in the country rocks compared to 0.93 in the xenoliths). It should be noted that the position of Al is rather inaccurate because small amounts should enter the melts before or with K, Na and Ca. Fig. 19 shows good agreements in the trends of the major, but not the trace elements with magmatic crystallization, with Ti, P and Zr showing the largest disagreement. This is attributed to the small sample size of the country rocks (only 13 samples for the trace elements), the gross inaccuracy of the calculations due to the large standard deviations, and the poor definition of some partition coefficients (e.g. Zr). In magmas however, zircon, apatite and ilmenite and titanite can crystallize before, with or after Mg-olivine and Ca-plagioclase (Read and Watson, 1962) and hence their order of fractionation in natural magmas is not fixed. If Zr, P and Ti are not considered, assuming they crystallize as accessory zircon, apatite and ilmenite and/or titanite respectively, the remaining trace elements show the same order of fractionation as is common in magmas (Fig. 19C).

The calculated degrees of partial melting, composition of the melts, CIPW norms, K_2O/Na_2O and mole $[Al_2O_3/(CaO+Na_2O+K_2O)]$ ratios (hereafter called A/CNK) are shown in Table 5 and can be compared with the actual values of the microgranite also given in Table 5.

Clearly, the actual microgranite and the calculated melt compositions are almost identical, even in their trace element contents. Particularly different is the lower Sr in the calculated melts which is due to some Sr in the xenoliths being derived from the gabbro magma (added in calcic plagioclase) for which no allowance has been made. The CIPW norms also show very good agreement. Both the calculated melts and the sill can be seen to consist of very similar proportions of normative quartz, orthoclase and plagioclase (albite+anorthite), consistent with the mineralogy. The A/CNK and K_2O/Na_2O also show very good agreement and both agree with S-type granites (Chappell and White, 1974). Likewise, as dealt with later, the Sr isotopes in the microgranite sill at 490 Ma match those of the metasediments.

The *REE* distribution in the microgranite (Fig. 12D) is similar to that in many granites (e.g. Harmon *et al.*, 1984) and matches well with the patterns of the country rock (Fig. 12A) and hornfelses (Fig. 12B) with a similar slightly negative Eu anomaly.

Overall then, the microgranite represents magma produced nearly *in situ* by melting, and segregated into a planar zone from which it could have been fed upwards to generate a small pluton.

Cashel leucosomes

Throughout a wide area of metasediment fringing the Connemara intrusive rock complex (Leake, 1989) there are pods and veins of leucosomes with paleosomes and it seems possible that these leucosomes might represent melt material approaching the microgranite in composition. The Cashel leucosomes are typically concordant, less than one metre wide and up to 5 m long. They are however trondhjemites and consist of quartz, plagioclase (An_{0-40}) and very rare orthoclase with biotite, garnet, sillimanite, andalusite, cordierite, zircon, apatite and secondary muscovite, sericite and occasionally prehnite.

Garnets in the leucosomes have the same chemical composition as those from the restites and are fractured and rich in quartz, sillimanite and biotite inclusions, which suggests they are xenocrystic. Much of the biotite is also believed to

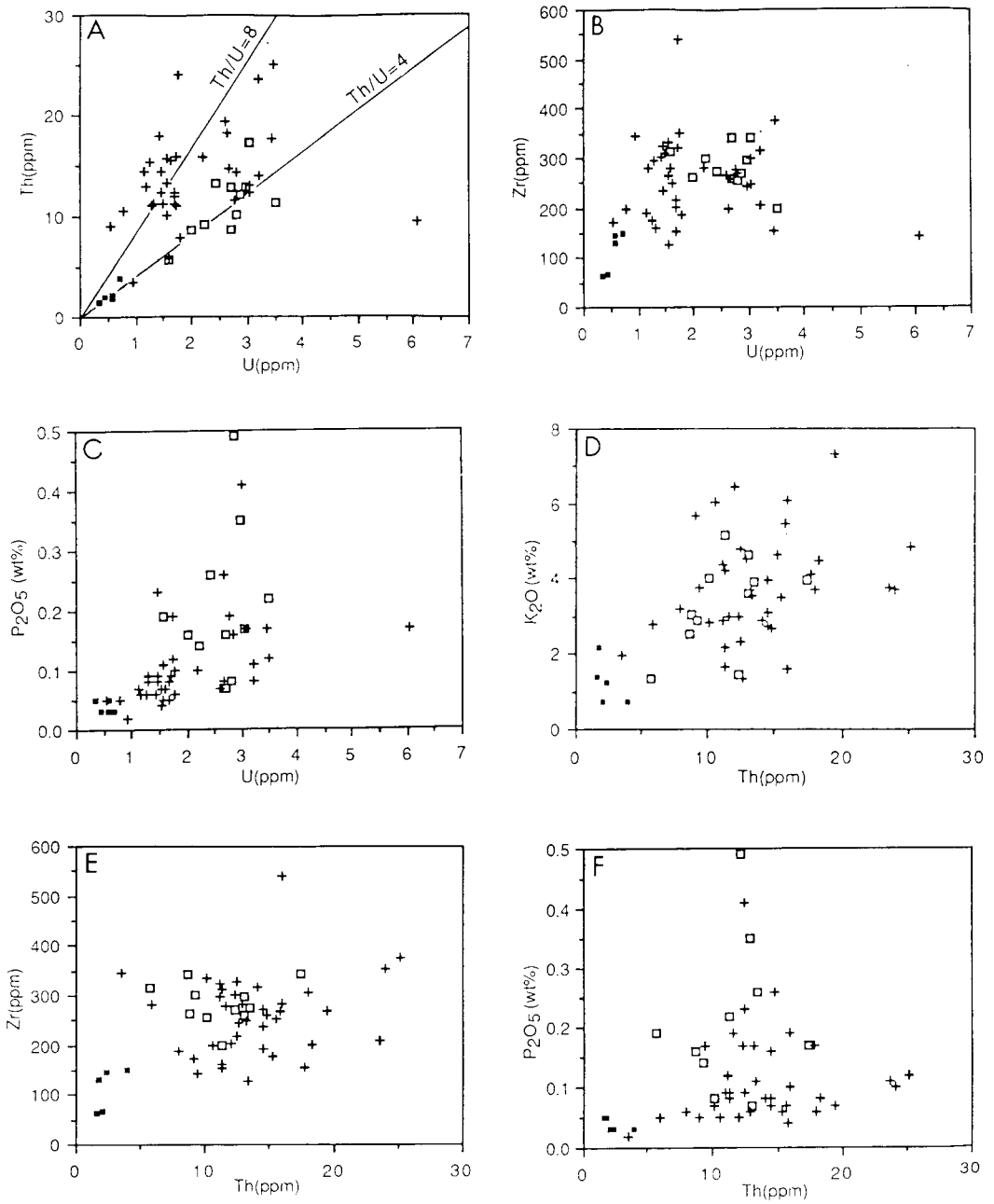

FIG. 17. Scatter diagrams for the metasediments of (A) U *vs.* Th, (B) U *vs.* Zr, (C) U *vs.* P_2O_5, (D) Th *vs.* K_2O, (E) Th *vs.* Zr, (F) Th *vs.* P_2O_5. Note the rise of the Th/U ratios with hornfelsing which then fall in the pelitic xenoliths to values similar to those in the country rocks. Open squares, unhornfelsed pelites; crosses, hornfelsed pelites; filled squares, pelitic xenoliths.

Table 5: Calculated melt compositions and their CIPW norms, A/CNK ratios. The actual composition of the microgranite sill is also given for comparison.

	1	2	3		4	5	6
	x	x	x	σ			
SiO_2	56.70	20.63	69.65	0.77	67.34	70.57	70.77
TiO_2	1.33	2.42	0.60	0.02	1.01	0.91	0.90
Al_2O_3	20.33	36.28	14.87	0.33	15.62	14.21	14.12
Fe_{tot}	9.59	28.14	3.10	0.32	4.12	2.46	2.34
MnO	0.23	0.17	0.07	0.05	0.25	0.25	0.25
MgO	3.42	7.39	1.52	0.38	2.25	1.89	1.87
CaO	1.99	2.94	1.86	0.42	1.71	1.62	1.62
Na_2O	2.31	1.09	2.97	0.26	2.67	2.78	2.80
K_2O	3.90	0.90	5.11	0.27	4.78	5.05	5.07
P_2O_5	0.20	0.04	0.23	0.03	0.25	0.26	0.26
Total	100	100	100		100	100	100
Cr	109	388	21*	2	23	1	0
Ni	48	173	3*	0.8	8	0	0
Co	24	101	1*	0.8	0	6	0
Ga	27	74	18*	0.7	13	9	9
Sr	242	596	219†	14	132	104	102
Zr	272	120	369*	20	320	332	332
Ba	891	658	833*	30	964	982	983
Pb	117	35	151†	8	143	149	150
Qz			27.08	3.71	27.20	29.52	29.55
Or			30.17	1.60	28.25	29.84	29.96
Al			25.11	2.17	22.59	23.52	23.69
An			7.54	2.17	6.85	6.34	6.34
Hyp			3.78	0.94	5.60	4.70	4.65
Ap			0.51	0.08	0.58	0.60	0.60
Cor			1.60	0.95	3.54	1.84	1.70
Ru			0.56	0.08	1.01	0.91	0.90
Sp			0.07	0.17	0	0	0
A/CNK			1.09	0.09	1.23	1.11	1.09
K_2O/Na_2O			1.70	0.11	1.79	1.82	1.81

Key to table 5

1 is the average of 47 country rock pelites (Table 2) recalculated to 100%
2 is the average of 9 pelitic xenoliths recalculated to 100%
3= average of 7 microgranites (one from Leake 1970, two from Jagger 1985, Laouar 1988 and this work) recalculated to 100% with standard deviation, σ
4 to 6 = melt compositions extracted from the average of 9 pelitic xenoliths calculated using Co, Ni and Cr respectively in which the degrees of partial melting possible are 77.2%, 42.2% and 71.9% respectively.
A/CNK= mole[Al_2O_3/($CaO+Na_2O+K_2O$)]
Fetot as Fe_2O_3
* average of four analyses only
† average of six analyses only
Note that the CIPW norms are calculated for the microgranite sill and the estimated melts only.

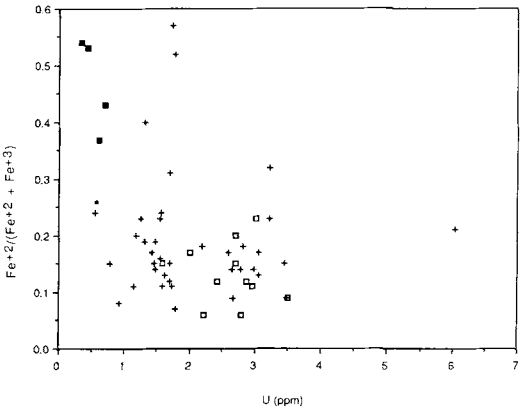

FIG. 18. U *vs.* $Fe^{3+}/(Fe^{3+} + Fe^{2+})$ for the metasediments.

have derived from the restites because the biotite–sillimanite intergrowth seen in the leucosomes is a common feature in the restites. However, many large red biotites are not intergrown and are more concentrated at the restite–leucosome contacts and hence are believed to have grown primarily from the melts. Andalusite is rare, commonly converted to shimmer aggregates and may be magmatic in part but the argument of Barber and Yardley (1985) that andalusite has grown from the melts because it is only found in the leucosomes is incorrect as it is found in both the restites and leucosomes. Cordierite is very rare and when found it occurs as small crystals usually partly pinitized. In contrast to cordierite from the restites, those from the leucosomes are almost free of biotite, sillimanite and quartz inclusions which suggests that at least some of cordierite crystallized in the leucosomes.

The chemical analysis of eight stromatic and schlieren and six quartz-rich leucosomes are statistically summarized in Table 6. Fig. 20 illustrates Harker-type diagrams which show SiO_2 to exhibit negative correlations with Al_2O_3, TiO_2, Fe_{tot} (as Fe_2O_3), K_2O and Na_2O. The negative correlation of SiO_2 with K_2O and Na_2O excludes the leucosomes from being late differentiated magmatic injections.

The *REE* are lower in the leucosomes than the microgranite or the hornfelses (Fig. 12B and D) and a pronounced positive Eu anomaly occurs in all leucosomes. It has been argued above that the positive Eu anomaly in the strongly melted xenoliths is due primarily to the extraction of a granitic melt from them and hence if the leucosomes were derived purely by partial melting from their corresponding restites, they should also have negative Eu anomalies like the microgranite (Fig. 12D) which is not the case. Mass balance calculations, Sr isotopes and the spacial association with the metasediments show the leucosomes to have been derived from the metasediments (see below). The positive Eu anomaly indicates that a significantly different process operated from that which produced the microgranite. Abundant xenocrystic plagioclase might explain the Eu anomaly but

Table 6: Summary statistics of the Connemara leucosomes

	1		2		3	
	x	σ	x	σ	x	σ
SiO_2	71.31	2.88	87.42	4.71	66.48	5.10
TiO_2	0.25	0.16	0.11	0.11	0.68	0.33
Al_2O_3	15.16	1.46	6.18	2.75	16.28	2.15
Fe_2O_3	0.56	0.43	0.25	0.16	1.28	0.49
FeO	1.60	0.91	0.72	0.48	3.39	1.45
MnO	0.03	0.01	0.02	0	0.07	0.03
MgO	0.82	0.61	0.24	0.27	1.47	0.57
CaO	2.15	0.60	0.82	0.61	2.10	0.47
Na_2O	3.67	1.78	1.39	1.0	3.34	0.62
K_2O	1.66	0.88	1.01	0.38	2.14	0.56
P_2O_5	0.22	0.07	0.08	0.06	0.19	0.10
Rb	53	33	32	17	68	.20
Ba	376	151	270	90	553	302
La	15	10	8	4	36	14
Ce	19	6	19	6	77	27
Y	16	12	6	4	24	7
Zr	42	37	55	105	139	43
Sr	274	157	108	82	304	95
Ga	17	5	7	2	18	3
Ni	8	5	3	4	25	13
Co	3	4	2	3	-	-
Cr	6	5	5	7	54	26

1= average of 8 stromatic and schlieren leucosomes
2= average of 6 quartz-rich leucosomes
3= average of 21 leucosomes from eastern Connemara (Barber 1985)
— not determined

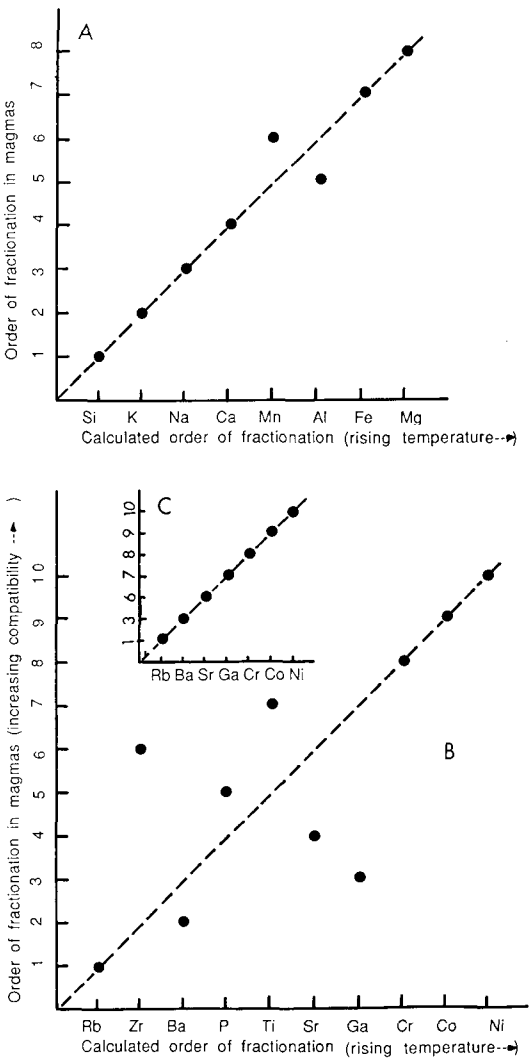

FIG. 19 (A–C). Order of fractionation in magmas versus the calculated order of fractionation of the elements in the Cashel thermal aureole. In A, 1 = Si, 2 = K, 3 = Na, 4 = Ca, 5 = Mn, 6 = Al, 7 = Fe, 8 = Mg. In B and C, 1 = Rb, 2 = Zr, 3 = Ba, 4 = P, 5 = Ti, 6 = Sr, 7 = Ga, 8 = Cr, 9 = Co, 10 = Ni.

Fig. 14C and D excludes plagioclase as the only cause for the Eu anomaly. Fractional crystallization which can result in a positive Eu anomaly (McCarty and Kable, 1978; Sawyer and Barnes, 1988), could not be significant on the scale required in such small leucosome patches. Other factors which might have affected Eu include changing oxygen fugacity and melting (Sun *et al.*, 1974), changing of the melt composition (Fraser, 1975), the presence of chloride and fluoride in the fluid phase during melting (Flynn and Burnham, 1978) and metamorphic segregation before melting. Volatile-rich fluids and segregation before substantial melting are believed the strongest influencing factors among the Connemara samples.

At the deduced temperatures of over 700 °C at 4–5 kbar with high water activity (biotite presence in the hornfelses), incipient melting will occur (Johannes, 1985). The fact that the leucosomes and their restites are generally K-feldspar free is not evidence against partial melting as Johannes (1985), Vielzeuf and Holloway (1988) and Le Breton and Thompson (1988) have shown. Rather, it suggests that escape of much of the K-rich, more evolved granitic-like melt has taken place leaving behind the 'failed granite' material of Le Breton and Thompson (1988), K-feldspar-free leucosomes are widespread throughout many high-grade metamorphic terranes such as central Massachusetts (Tracy, 1985), NW Scotland in the Moine rocks (Barr, 1985), Skagit Gneiss migmatites, Washington (Yardley, 1978).

An attempt has been made to calculate the original compositions of the leucosome melts produced by anatexis in order to compare with the

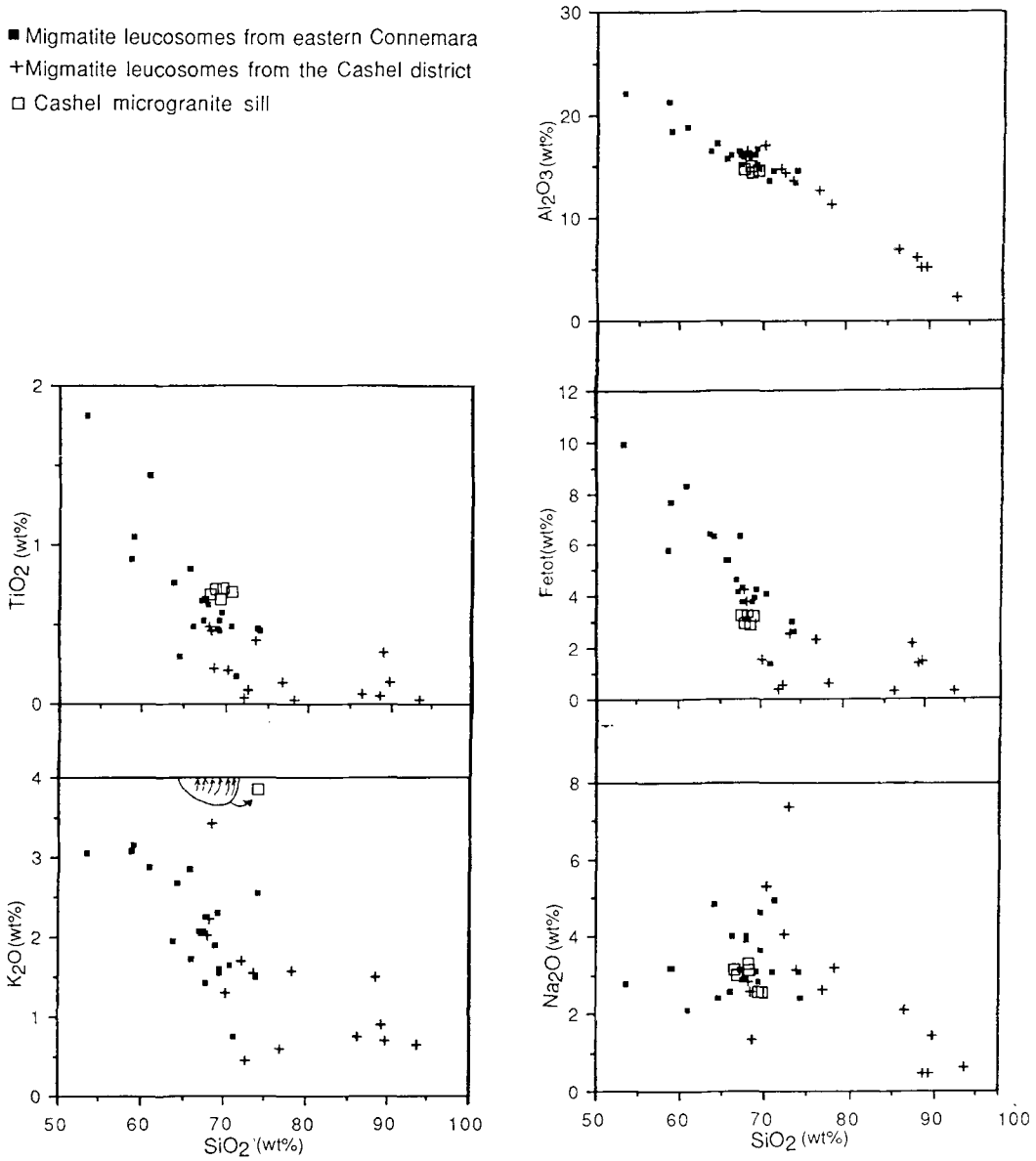

FIG. 20. Harker-type diagrams of the Connemara leucosomes. Data from eastern Connemara from Barber (1985) are also shown.

microgranite sill. Using the method as with the hornfelses but treating the pelitic paleosomes as the restite material, Table 7 shows the calculated melts derived from between 18 and 38% partial melting generally agree with the average leucosomes although some elements such as K and Na show significant differences. The quartz-rich leucosomes are also clearly different from melts calculated at low degrees of partial melting (10%) which therefore confirms that much of the leucosome material is not simply a complete sample of the results of partially melting pelite.

Despite the numerous theoretical and experimental studies relevant to granite genesis (e.g. Tuttle and Bowen, 1958; Luth *et al.*, 1964), very few have been undertaken on naturally occurring

Table 7. Degrees of partial melting and melt compositions derived from the Cashel hornfelsed pelites with experimental comparisons.

	A	
	min.	*max*
Cr	24.3	31.2
Ni	29.4	44.5
Co	20.0	22.3

	1		2		melts at the degree of partial melting stated				
	x	σ	x	σ	10%	20%	30%	40%	50%
SiO_2	69.35	4.54	88.91	4.71	81.45	72.06	67.40	63.40	61.10
TiO_2	0.56	0.31	0.1	0.11	0	0	0.52	0.80	0.98
Al_2O_3	16.48	2.00	6.28	2.75	4.26	13.30	15.83	17.77	18.63
Fe_{tot}	4.39	1.97	1.07	0.69	0	0	3.05	5.39	6.78
MnO	0.06	0.02	0.02	0	0.72	0.50	0.39	0.33	0.30
MgO	1.31	0.60	0.25	0.27	0	1.55	2.36	2.73	2.96
CaO	2.16	0.65	0.83	0.61	5.10	3.72	3.06	2.66	2.44
Na_2O	3.49	1.07	1.41	1.0	5.24	3.96	3.34	2.96	2.74
K_2O	2.04	0.70	1.03	0.38	2.61	3.48	3.71	3.67	3.81
P_2O_5	0.16	0.14	0.09	0.06	0.62	0.43	0.34	0.29	0.26
	100		100		100	100	100	100	100

	3	4	5	6	7	σ
SiO_2	64.5	74.1	72.6	66.2	69.98	0.77
TiO_2	0.80	0.5	0.1	0.8	0.59	0.03
Al_2O_3	18.2	14	16.7	18	14.93	0.33
Fe_{tot}	6.2	3.6	1.7	5	2.98	0.04
MgO	2.1	1	0.7	1.6	1.53	0.38
CaO	2.8	1.8	2.9	2.7	1.87	0.43
Na_2O	1.7	1.1	1.6	1.8	2.99	0.25
K_2O	3.7	3.9	3.7	3.9	5.13	0.27
	100	100	100	100	100	

A= The calculated minimum and maximum percentages of melt produced from the difference in composition between the average of 47 country rock pelites and 104 hornfelsed pelites using Cr, Ni and Co individually.

1= Average of 29 leucosomes (21 from Barber, 1985 and 8 this work), with standard deviation σ

2= Average of 6 quartz-rich leucosomes with standard deviations, σ

3= Starting composition of pelitic glass of Green (1976)

4= Melt results of Green at 4Kb, 780°C, 124 hours, 5% water added

5= Melt results of Green at 10Kb, 820°C, 95 hours, 5% water added

6= Melt results of Green at 10Kb, 1040°C, 2.5 hours, 5% water added

7= Average of 7 microgranite sill analyses with standard deviations, σ

metasedimentary rocks at the appropriate *P–T* conditions (e.g. Green, 1976; Winkler, 1976, 1979). From the studies of Tracy (1978), Abbot and Clarke (1979), Thompson and Tracy (1979), Clemens and Wall (1981), Thompson (1982), Manning (1981), Pichavant (1981), Manning and Pichavant (1983) and others, it is now understood that a wide variety of granitic compositions can be generated from pelitic rocks due to differing *P–T* conditions, the original composition of the rocks, the composition and amount of the fluids present at the time of melting, and that the melts generated need not correspond to the 'minimum melt' composition.

The A/CNK, CIPW, normative corundum, Qz:Ab:Or ratios (recalculated to 100%) of the leucosomes as given in Table 8, suggest S-type granites for the Cashel leucosomes, as defined by Chappell and White (1974). The composition of the starting synthetic glass and the results of the experiments of Green (1976) are compared in Table 7 with the composition of the Cashel metasediments, leucosomes and microgranite sill. The most applicable resuilts of Green's experiments to the Cashel leucosomes are those produced at 780 °C and 4 kbar as these *P–T* conditions are similar to those which prevailed in the Cashel area. It is clear that although the experimentally derived glass and the naturally occurring Cashel leucosomes tend to agree in many elements, there is a significant tendency for the leucosomes to be poorer in Si and K but richer in Na compared to the experimental results. The Cashel microgranite sill which was derived from highly melted metasediments relative to the leucosomes, is richer in Na and K but poorer in Si compared to the composition of the glass which suggests that the differences between the Cashel microgranite sill and leucosomes on the one hand and Green's experimentally derived glass on the other is the result of differing composition of the starting material, differing degrees of partial melting, *P–T* conditions and possibly different fluid conditions.

As Fig. 21 shows, most of the microgranite samples plot within the anatectic field of Winkler (1979) but the leucosomes are far more variable in terms of their Qz:Ab:Or ratios with only few points plotting within the anatectic field. This disagreement cannot be the result of the anatectic field being produced at 2 kbar compared with 4–5 kbar in the Cashel area because increased pressure would shift the anatectic field towards the Ab apex (direction of arrow). These trends are probably caused by the leucosomes not being a complete and unchanged partial melt or in part being metamorphic segregations.

Five leucosomes including one restite-leucosome pair were analysed for Rb, Sr and Rb–Sr isotopic composition and are shown in Table 8. The restite–leucosome pair yields an age of 544 m.y. which is higher than the average of 442 ± 25 m.y. obtained from 7 restite–leucosome pairs (Barber, 1985). The $(^{87}Sr/^{86}Sr)_{490}$ of the Cashel leucosomes fall within the range of between 0.71576 and 0.72365, similar to leucosomes from eastern Connemara (Barber, 1985) suggesting a similar origin from Dalradian metasediments. The leucosomes and Cashel microgranite have $(^{87}Sr/^{86}Sr)_{490}$ values of roughly 0.718 which is different from 0.710 and 0.712 of the quartz-diorite and K-feldspar intrusive gneisses. Likewise the $(^{87}Sr/^{86}Sr)_{490}$ of the metagabbros, which are typically 0.708 to 0.712 (Jagger, 1985), are quite distinctly lower than either the microgranite or the leucosomes, so there is no possibility of the leucosomes being injected gneiss from the intrusive gneiss complex. It is not therefore clear

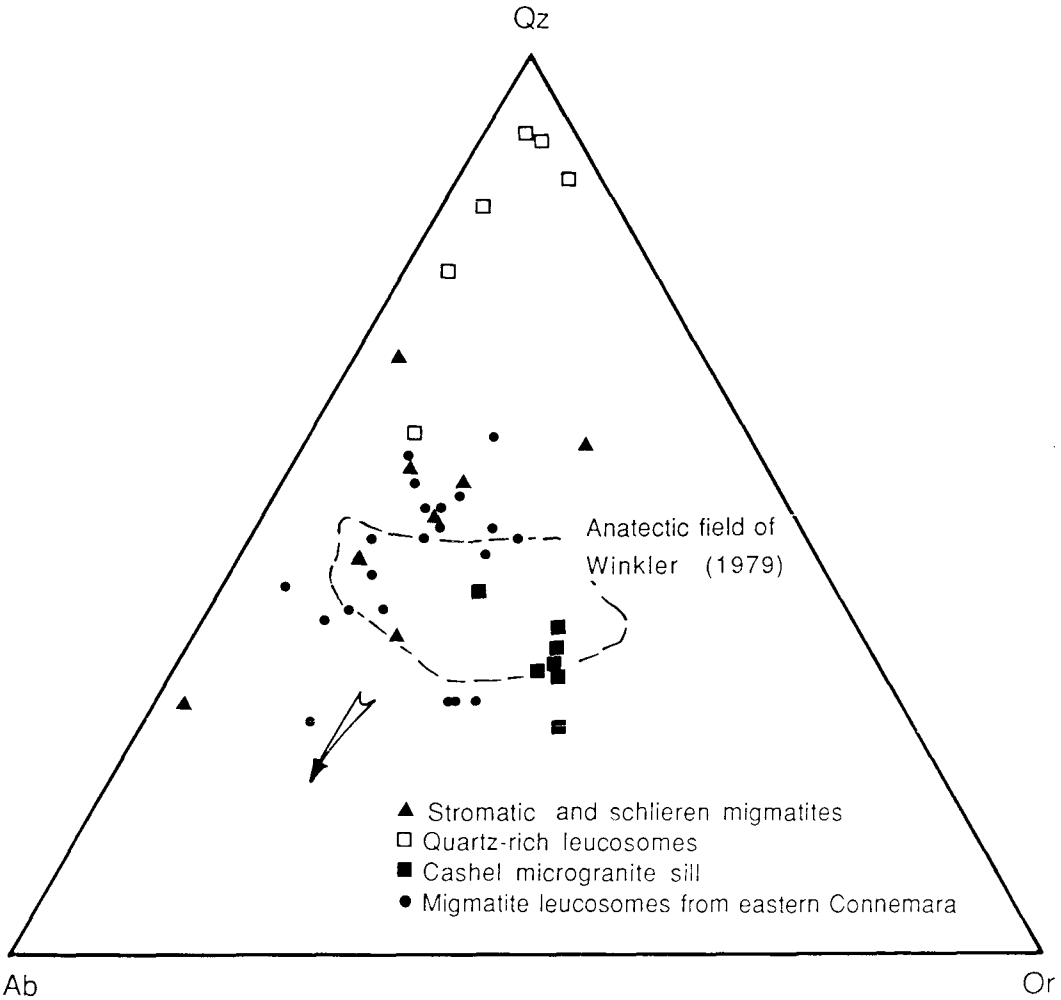

FIG. 21. Qz–Ab–Or triangle diagram for the Connemara leucosomes and Cashel microgranite sill. Arrow indicates shifting of the Qz:Ab:Or ratios with rising pressure. Data from eastern Connemara from Barber (1985) are also shown.

what relevance the leucosomes have for the Cashel microgranite.

Conclusions

(1) The aureole temperature around the Cashel body exceeded 850 °C at pressures of about 4.05 ± 0.2 kbar with a widespread zone with temperatures in excess of 700 °C.

(2) The elements investigated were fractionated in the aureole practically in the same way as occurs in reverse in naturally crystallizing magmas, indicating that fractional melting was the operative process as is demonstrated by the composition of the strongly hornfelsed metasediments which have suffered loss Si, K, Na, Al, etc.

(3) The *REE* were both removed and fractionated with Eu being left in the crystal phases in preference to the outgoing melts, giving increasing positive Eu anomalies. These trends are the result of removing a granitic melt and recrystallization and/or melting of some key minerals, particularly zircon and apatite.

(4) U, and at relatively later stages Th, were fractionated into the melts as a result of many mechanisms: recrystallization of minerals particularly zircon and apatite, changing textural relationships, melting of the main carriers of U and Th

Table 8: Molecular ACNK ratios, normative corundum(C) and normative quartz-albite: orthoclase and Sr isotope data of the Cashel leucosomes and microgranite sill.

stromatic and schlieren leucosomes					quartz-rich leucosomes		
	Qz:Ab:Or	C	A/CNK		Qz:Ab:Or	C	A/CNK
Y11	53:29:18	6.79	1.68	Y5	75:20:5	0.40	0.99
Y12	36:55:9	3.21	1.68	Y40	58:31:11	1.75	1.38
Y42	57:15:28	8.07	1.97	Y43	86:4:10	3.69	2.20
Y44	45:42:13	2.22	1.14	Y60	83:13:4	2.05	1.63
Y68	66:29:5	2.19	1.20	Y65	90:6:4	0	0.60
Y69	28:69:3	0	0.92	Y78	89:5:6	2.68	1.97
Y71	49:34:17	5.48	1.46				
Y72	54:34:12	2.34	1.19				

Isotopic data

	Rb	Sr	$^{87}Rb/^{86}Sr$	$(^{87}Sr/^{86}Sr)_P$	$(^{87}Sr/^{86}Sr)_{490}$
Y42L	118.5	153.5	2.2410	0.73936±6	0.72403
Y65L	15.84	48.06	0.9558	0.72851±8	0.72197
Y68L	14.53	462.8	0.0909	0.71756±6	0.71693
Y68R	103.1	482.3	0.6193	0.72166±4	0.71742
Y69L	13.73	497.3	0.0799	0.71759±10	0.71704
J041	149.5	208.1	2.0848	0.73523±3	0.72081
J043	141.3	221.8	1.8471	0.73331±3	0.72054

R= restite (this work)
L= Leucosomes (this work)
J= Microgranite sill (Jagger 1985)
p= present

particularly biotite, zircon, apatite and cordierite, incipient partial melting with U and to a lesser extent Th being preferentially fractionated into the melts during dehydration and decarbonation.

(5) The S-type Cashel microcline microgranite still represents the segregated material melted out of the strongly heated and partially melted Dalradian metasediments, thus providing an example of the method of production of an S-type granite and the environment of interaction between mid-crustal rocks and mantle-derived intrusive gabbros. A distinctive metasedimentary Sr isotope ratio is preserved.

(6) The Cashel leucosomes, although clearly derived from the Dalradian metasediments, are significantly modified partial melts or metamorphic segregations (or both) and do not have compositions similar to the microgranite.

Acknowledgements

Drs A. B. Mackenzie, J. E. Whitley and J. Hamilton of the S.U.R.R.C. are thanked for their help with U and Th analyses using FT and INAA and for the Sr isotope analyses. Dr N. Walsh, J. Barker and A. Warren of the R.H.B.C, London are thanked for their assistance with the REE analyses. Drs M. D. Jagger and J. P. Barber and Mr R. Laouar kindly allowed reference to unpublished results. The Algerian government is particularly thanked for a research scholarship for the first author. Dr B. W. D. Yardley and an unknown referee made substantial scientific improvements.

References

Abbot, R. N. and Clarke, D. B. (1979) Hypothetical liquidus relationships in the subsystem Al_2O_3-FeO-MgO projected from quartz, alkali feldspar and plagioclase for $a(H_2O) \leq 1$. *Can. Mineral.* **17,** 549–60.

Ahmed-Said, Y. (1988) *The geochemistry of thermal aureoles at Cashel, Co Galway, and Comrie, Perthshire.* Ph.D thesis, Univ. of Glasgow (unpub.).

Barber, J. P. (1985) *High-grade metamorphism and melting in the Dalradian of eastern Connemara, Ireland.* Ph.D thesis, Univ. of East Anglia (unpub.)

—— and Yardley, B. W. D. (1985) Conditions of high grade metamorphism in the Dalradian of Connemara, Ireland. *J. Geol. Soc. Lond.* **142,** 87–96.

Barr, D. (1985) Migmatites in the Moines. In *Migmatites* (Ashworth, J. R., ed.). Blackie, Glasgow, 225–64.

Bowen, N. L. (1928) *The evolution of igneous rocks.* Princeton University Press, 332 pp.

Carslaw, H. S. and Jaeger , J. C. (1947) *Conduction of heat in solids.* Oxford Univ. Press, 386 pp.

—— (1959) Ibid., 2nd ed., 510 pp.

Chappell, B. W. and White, A. J. R. (1974) Two contrasting granite types. *Pacific geol.* **8,** 173–4.

Clemens, J. D. and Wall, V. J. (1981) Origin and crystallization of some peraluminous (S-type) granitic magmas. *Can. Mineral.* **19,** 111–31.

Dallmeyer, R. D. (1974) The role of crystal structure in controlling the partitioning of Mg and Fe^{+2} between coexisting garnet and biotite. *Am. Mineral.* **59,** 201–3.

Drury, S. A. (1978) *REE* distributions in high-grade Archean gneiss complex in Scotland: Implications for the genesis of ancient sialic crust. *Precambrian Res.* **7,** 237–57.

Evans, B. W. (1964) Fractionation of elements in the pelitic hornfelses of the Cashel-Lough Wheelaun intrusion, Connemara, Eire. *Geochim. Cosmochim. Acta*, **28,** 127–56.

—— and Leake, B. E. (1970) The geology of the Toombeola district, Connemara, Co. Galway. *Proc. Roy. Irish Acad.* **70B,** 105–39.

Ferry, J. M. and Spear, F. S. (1978) Experimental calibration of the partitioning of Fe and Mg between biotite and garnet. *Contrib. Mineral. Petrol.* **66,** 113–17.

Flynn, R. T. and Burnham, C. W. (1978) An experimental determination of rare earth partition coefficients between a chloride containing vapor phase and silicate melts. *Geochim. Cosmochim. Acta,* **42,** 685–701.

Fraser, D. H. (1975) Activities of trace elements in silicate melts. Ibid. **39,** 1525–30.

Ghent, E. D. (1976) Plagioclase–garnet–Al_2SiO_5–quartz: a potential geobarometer–geothermometer. *Am. Mineral.* **61,** 710–14.

—— Robbins, D. B. and Stout, M. Z. (1979) Geothermometry, geobarometry and fluid compositions of metamorphosed calc-silicates and pelites, Mica Creek, British Columbia. Ibid. **64,** 874–85.

Grant, J. A. and Weiblen, P. W. (1971) Retrograde

zoning in in garnet near the second sillimanite isograde. *Am. J. Sci.* **270,** 281–96.

Grauert, B., Seitz, M. G. and Soptrajanova, G. (1974) Uranium and lead gain of detrital zircon studied by isotopic analyses and fission track mapping. *Earth Planet. Sci. Lett.* **21,** 389–99.

Green, T. H. (1976) Experimental generation of cordierite- or garnet-bearing granitic liquids from a pelitic composition. *Geol.* **4,** 85–8.

Harmon, R. S., Halliday, A. N., Clayburn, J. A. P. and Stephens, W. E. (1984) Chemical and isotopic systematics of the Caledonian intrusions of Scotland and northern England: a guide to magma source region and magma-crust interaction. *Phil. Trans. Roy. Soc. Lond.* **A310,** 709–42.

Heier, K. S. and Adams, J. A. S. (1965) Concentration of radioactive elements in deep crustal material. *Geochim. Cosmochim. Acta,* **29,** 53–61.

Henderson, P. (1984) General geochemical properties and abundances of the rare earth elements. In *Rare Earth Element Geochemistry* (Henderson, P., ed.) *Developments in Geochemistry,* **2.** Elsevier, Amsterdam, 1–13.

Hodges, K. V. and Spear, F. S. (1982) Geothermometry, geobarometry and the Al_2SiO_5 triple point at Mt. Moosilauke, New Hampshire, *Am. Mineral.* **67,** 1118–34.

Holdaway, M. J. and Lee, S. M. (1977) Cordierite stability in high-grade pelitic rocks based on experimental, theoretical and natural observations. *Contrib. Mineral. Petrol.* **63,** 175–98.

Huppert, H. E. and Sparks, R. S. J. (1988) The generation of granitic magmas by intrusion of basalt into continental crust. *J. Petrol.* **29,** 599–624.

Indares, A. and Martignole, J. (1985) Biotite–garnet geothermometry in granulite facies: the influence of Ti and Al in biotite. *Am. Mineral.* **70,** 272–8.

Jaeger, J. C. (1958) The temperature in the neighbourhood of a cooling intrusive sheet. *Am. J. Sci.* **255,** 306–18.

—— (1959) Temperature outside a cooling intrusive sheet. Ibid. **257,** 44–54.

Jagger, M. D. (1985) *The Cashel district of Connemara, Co Galway, Eire: an isotopic study.* Ph.D. thesis, Univ. Glasgow (unpub.).

—— Max, M. D., Aftalion, M., and Leake, B. E. (1988) U-Pb zircon ages of basic rocks of Cashel, Connemara, Western Ireland. *J. Geol. Soc. Lond.* **145,** 645–8.

Jenkin, J. R. T. (1988) *Stable isotope studies in the Caledonides of SW Connemara, Ireland.* Ph.D. thesis, Univ. Glasgow (unpub).

Johannes, W. (1985) The significance of experimental studies for the formation of migmatites. In *Migmatites* (Ashworth, J. R., ed.) Blackie, Glasgow, 36–85.

Laouar, R. (1988) *A sulphur isotope study of the Caledonian granites of Britain and Ireland.* M.Sc. thesis, Univ. Glasgow (unpub.).

Leake, B. E. (1958*a*) The Cashel Lough Wheelaun intrusion, Co Galway, Ireland. *Proc. Roy. Irish Acad.* **59B,** 155–203.

—— (1958*b*) Composition of pelites from Connemara, Co, Galway, Ireland. *Geol. Mag.* **95,** 281–96.

—— (1970) The fragmentation of the Connemara basic and ultrabasic intrusions. In *Mechanisms of igneous intrusion* (Newall, G. and Rast, N., eds.) *Geol. J. Special Issue,* no. 2, 103–22.

—— (1989) The metagabbros, orthogneisses and paragneisses of the Connemara complex, Western Ireland. *J. Geol. Soc. Lond.* **146,** 575–96.

—— and Skirrow, G. (1960) The pelitic hornfelses of the Cashel-Lough Wheelaun intrusion, Co. Galway, Eire. *J. Geol.* **68,** 23–40.

Le Breton, N. and Thompson, A. B. (1988) Fluid-absent (dehydration) melting of biotite in metapelites in the early stages of crustal anatexis. *Contrib. Mineral. Petrol.* **99,** 226–37.

Luth, W. C., Jahns, R. H., and Tuttle, O. F. (1964) The granite system at pressures of 4 to 10 Kbs. *J. Geophy. Res.* **69,** 759–73.

Manning, D. A. C. (1981) The effect of fluorine on liquidus phase relationships in the system Qz:Ab:Or with excess water at 1 Kb. *Contrib. Mineral. Petrol.* **76,** 206–15.

—— and Pichavant, M. (1983). The role of fluorine and boron in the generation of granitic melts. In *Migmatities, melting and metamorphism* (Atherton, M. P. and Gribble, C. D., eds.) Shiva, Orpington, 94–109.

McCarty, T. S. and Kable, E. J. C. (1978) On the behaviour of the rare-earth elements during partial melting of granitic rocks. *Chem. Geol.* **22,** 21–9.

Newton, R. C. and Haselton, H. T. (1981) Thermodynamics of the garnet-plagioclase–Al_2SiO_5–quartz geobarometer. In *Thermodynamics of minerals and melts* (Newton, R. C., Navrotsky, A., and Wood, B. J., eds.) Springer-Verlag, New York, 131–47.

Pichavant, M. (1981) An experimental study of the effect of boron on a water saturated haplogranite at 1 Kb vapour pressure. Geological applications. *Contrib. Mineral Petrol* **76,** 430–9.

Read, H. H. and Watson, J. (1982) *Introduction to geology,* **1.** Macmillan.

Rogers, N. W. (1977) Granulite xenoliths from Lesotho Kimberlites and the lower continental crust. *Nature, Lond.* **270,** 681–4.

Sawyer, E. W. and Barnes, S.-J. (1988) Temporal and compositional differences between subsolidus and anatectic migmatite leucosomes from the Quetico metasedimentary belt, Canada. *J. Metam. Petrol.* **6,** 437–50.

Senior, A. and Leake, B. E. (1978) Regional metamorphism and the geochemistry of the Dalradian metasediments of Connemara, western Ireland. *J. Petrol.* **19,** 585–625.

Sun, C. O., Williams, R. J. and Sun, S. S. (1974) Distribution coefficients of Eu and Sr for plagioclase-liquid and clinopyroxene-liquid equilibria in oceanic ridge basalt: an experimental study. *Geochim. Cosmochim. Acta,* **38,** 1415–33.

Taylor, S. R. and McLennan, S. M. (1955) *The continental crust: its composition and evolution.* Blackwell Scientific Publications, Oxford, 312 pp.

Thompson, A. B. (1976) Mineral reactions in pelitic rocks: II. Calculation of some *P–T–X* (Fe–Mg) phase relations. *Am. J. Sci.* **276,** 425–54.

—— (1982) Dehydration melting of pelitic rocks and the generation of H_2O-undersaturated granitic liquids. Ibid. **282,** 1567–95.

—— and Tracy, R. J. (1979) Model systems for anatexis of pelitic rocks. II. Facies series melting and reactions in the system $KAlO_2$–$NaAlO_2$–Al_2O_3–SiO_2–H_2O. *Contrib. Mineral. Petrol.* **70,** 429–38.

Tilley, C. E. (1924) Contact metamophism in the Comrie area of the Perthshire Highlands. Q. J. Geol. Soc. Lond. **80,** 22–71.

Tracy, R. J. (1978) High-grade metamorphic reactions and partial melting in pelitic schist, western-central Masschusetts. *Am. J. Sci.* **278,** 150–78.

—— (1985) Migmatite occurrences in New England. In *Migmatites* (Ashworth, J. R., ed.) Blackie, Glasgow, 204–24.

Treloar, P. J. (1981) Garnet–biotite–cordierite thermometry and barometry in the Cashel thermal aureole, Connemara, Ireland. *Mineral. Mag.* **44,** 183–9.

—— (1985) Metamorphic conditions in central Connemara, Ireland. *J. Geol. Soc. Lond.* **142,** 77–86.

Tuttle, O. F. and Bowen, N. L. (1958) Origin of granite in the light of experimental studies in the system $NaAlSi_3O_8$–$KAlSi_3O_8$–SiO_2–H_2O. *Mem. Geol. Soc. Am.* **74,** 173 pp.

Vielzeuf, D. and Holloway, J. R. (1988) Experimental determination of the fluid absent melting relations in the pelitic system. Consequences for crustal differentiation. *Contrib. Mineral. Petrol.* **98,** 257–76.

Wells, P. R. A. and Richardson, S. W. (1980) Thermal evolution of metamorphic rocks in the central Highlands of Scotland. In *The Caledonides of the British Isles—reviewed* (Harris, A. L., Holland, C. H. and Leake, B. E., eds.) Spec. Publ. Geol. Soc. London, **8,** 339–44.

Winkler, H. G. F. (1976) *Petrogenesis of Metamorphic Rocks,* 4th ed. Springer-Verlag, New York, 334 pp.

—— (1979) Ibid., 5th ed. Springer-Verlag. New York, 348 pp.

Yardley, B. W. D. (1978) Genesis of the Skagit Gneiss migmatities, Washington, and the distinction between possible mechanisms of migmatization. *Geol Soc. Am. Bull.* **89,** 941–51.

—— (1987) Discussion on the geochemistry of Dalradian pelites from Connemara, Ireland: New constraints on kyanite genesis and conditions of metamorphism. *J. Geol. Soc. Lond.* **144,** 679–80.

—— Leake, B. E. and Farrow, C. M. (1980) The metamorphism of Fe-rich pellites from Connemara, Ireland. *J. Petrol.* **21,** 365–99.

—— Barber, J. P. and Gray, J. R. (1987) The metamorphism of the Dalradian rocks of western Ireland and its relation to tectonic setting.. *Phil. Trans. Roy. Soc. Lond.* **321,** 243–70.

[*Manuscript received 27 January 1989: revised 20 September 1989*]